

C •

FCTUC FACULDADE DE CIÊNCIAS
E TECNOLOGIA
UNIVERSIDADE DE COIMBRA

DEPARTAMENTO DE
ENGENHARIA MECÂNICA

System Identification of a Radiant Ceiling Panel circuit and its surrounding environment

Submitted in Partial Fulfilment of the Requirements for the Degree of Master in
Mechanical Engineering in the speciality of Production and Project

Author

Daniel Pedrosa da Silva

Advisors

Adélio Manuel Rodrigues Gaspar

João Alexandre Dias Carrilho

Jury

President Professor Doctor Ricardo António Lopes Mendes
Professor of University of Coimbra

Vowel Professor Doctor Manuel Carlos Gameiro da Silva
Professor of Universidade of Coimbra

Advisor PhD Student João Alexandre Dias Carrilho
Assistant Professor of Universidade of Coimbra

Coimbra, July, 2015

Tudo o que é realmente grande e inspirador é criado pelo indivíduo que pode
trabalhar em liberdade.

Albert Einstein

Aos meus pais e à minha irmã.

ACKNOWLEDGEMENTS

The present work was accomplished with a lot of effort and a great dedication. The field of this thesis couldn't be better and all the developments were made with joy and enthusiasm. After all the good moments and barriers, this work became possible, in order to achieve a dream, which of course couldn't be reached without the collaboration and effort of some important people, and for those I recognize their role in my academic journey.

In first place, I thank to my co-advisor João Carrilho, for enhancing the developed work, but mostly because of his full-time dedication, motivation and availability. João Carrilho taught me a lot of interesting and helpful concepts, helped me in my daily tasks and presented me his commitment as an example to follow in the future.

I also thank Professor Adélio Gaspar for his interest on the work developments and his motivational attitude. Obviously his role as my teacher had a lot of influence when the moment of the thesis application arrived. As well as the role of Professor Manuel Gameiro, who taught the most interesting subject, at my point of view, with his incomparable knowledge of instrumentation and measurement.

My friends were also important to make this a reality, they stood by my side on the moments of non-progression or even when I accomplished great results. For those, a great "thank you".

Finally, bust most important, this couldn't be done without my family's support and effort. They fought for me every day and made me a better person, a better student and, definitely a better dreamer. A proud "thank you" to my mother Natália, sister Matilde and to the best mechanical engineer in the world: my father Adelino.

Abstract

The purpose of this work is to present a simple methodology and its results for the identification of a water driven radiant panel system on a typical university laboratory. Several works of numerical investigation have been done by other authors in order to identify the system characteristic parameters, and the thermal model approach presented in this work aims to simplify the response of the indoor climate to the radiant ceiling panels operation.

To this end, experimental work was performed which consisted in measuring the indoor variables such as the air, operative and mean radiant temperatures, in response to the input water temperature and the external conditions. Passing on a brief analysis on the thermal comfort and through a power output calculation procedure it was possible to obtain a thermal model that fits the behaviour of the air temperature, based on an energetic balance following a first order system response.

It was found that about 32 % of the energy of the radiant panels' hot water is directly transferred to the air. It was also possible to infer on the level of input energy and it was concluded that there is a tolerable difference between the mathematical model and the real response.

Keywords Radiant Heating, Radiant Panels, System Identification, PMV, Control, Thermal Model.

Resumo

O objetivo do presente trabalho é apresentar uma metodologia simples e seus resultados para a identificação de um sistema de painéis radiantes (com circulação de água) num laboratório típico. Vários trabalhos de investigação numérica têm sido realizados com o propósito de identificar os parâmetros característicos de sistema, e o modelo térmico apresentado neste trabalho pretende simplificar a resposta do clima interior ao funcionamento dos painéis radiantes.

Para que tal seja alcançado, foi elaborada uma atividade experimental que consistiu na medição de variáveis internas como a temperatura do ar, a operativa e a temperatura média radiante, em resposta à entrada da temperatura da água e às condições externas. Passando por uma breve análise de conforto térmico e através do cálculo da potência térmica, foi possível adquirir um modelo térmico que é fiel ao comportamento da temperatura do ar, baseado num balanço energético que segue a resposta de um sistema de primeira ordem.

Foi constatado que cerca de 32 % da energia da água quente dos painéis radiantes é diretamente transferida para o ar. Foi, também, possível inferir do nível de energia fornecida ao sistema e concluiu-se igualmente que existe uma diferença tolerável entre o modelo matemático e a resposta real.

Palavras-chave: Aquecimento Radiante, Painéis Radiantes, Identificação de Sistema, PMV, Controlo, Modelo Térmico.

Contents

LIST OF FIGURES	xi
NOMENCLATURE AND ACRONYMS	xiii
Nomenclature.....	xiii
Acronyms	xv
1. INTRODUCTION	1
1.1. State of the Art.....	1
1.1.1. Definition of Radiant Heating	1
1.1.2. History and Context.....	3
1.1.3. Radiant Panels	5
1.1.4. Studies on Radiant Panel Systems.....	9
1.2. Objectives and Motivation.....	11
1.3. The Existing Radiant Panels Installation	13
1.4. Operation of the Existing Radiant Panels	17
2. MATERIALS AND METHODS	19
2.1. Experimental Assembly	19
2.1.1. Introduction to System Identification	19
2.1.2. Instrumentation.....	20
2.1.3. Data Acquisition.....	23
2.1.4. Calibrations and Adjustments.....	24
2.1.5. Measurement Procedure and Calculation of Derived Quantities	25
3. RESULTS AND DISCUSSION.....	27
3.1. Preliminary Analysis.....	27
3.2. Effective Analysis.....	30
4. SYSTEM IDENTIFICATION	39
4.1. Estimating the Power Output of the Radiant Panels.....	39
4.2. Estimating the Laboratory Thermal Parameters	42
4.3. System Performance in terms of the Occupancy	46
5. CONCLUSIONS	51
BIBLIOGRAPHY	53
APPENDIX	55
A – Descriptors of Thermal Comfort	55
Plane Radiant Temperature	55
Mean Radiant Temperature	56
Operative Temperature	60
Dew-Point Temperature	61
Predicted Mean Vote and Predicted Percentage of Dissatisfied.....	61
B – Instrumentation Description	65
C – Calibrations and Adjustments	70

ANNEX A 73
ANNEX B 75
ANNEX C 77

LIST OF FIGURES

Figure 1.1. Example of beings' behaviour when looking for thermal comfort	1
Figure 1.2. Perceived temperature with radiant heating.....	2
Figure 1.3. Comparison between radiant panels and air heating systems.	3
Figure 1.4. Roman hypocaust.....	3
Figure 1.5. Examples of buildings with radiant ceiling panels.	4
Figure 1.6. Brands of radiant heating equipment.	4
Figure 1.7. Types of radiant heating equipment.....	5
Figure 1.8. The radiant ceiling panel typical structure (Adapted from: Zehnder ZBN).....	7
Figure 1.9. EAI skin disease symptom (Source: "Diseases of the Skin", James H. Sequeira, 1915).....	8
Figure 1.10. Location of radiant heating and cooling research projects.....	9
Figure 1.11. Simplified scheme of the radiant panel circuit.....	12
Figure 1.12. Scheme of the developed thesis work.....	13
Figure 1.13. Model of the laboratory of the experimental activity.....	14
Figure 1.14. The radiant ceiling panel circuit of the experimental activity.....	14
Figure 1.15. Structure of the Zehnder ZIP2 panels.	15
Figure 1.16. Water track on simplified opened circuit.	15
Figure 1.17. Bypass zone of the circuit.	16
Figure 1.18. First order response.....	17
Figure 1.19. Example of the input actuation for a set of a certain output value.....	18
Figure 2.1. Experimental assembly objective scheme.....	20
Figure 2.2. Wireless thermistor.	21
Figure 2.3. Thermistor vertical bar.....	22
Figure 2.4. Thermistor with aluminium foil protection.....	22
Figure 2.5. Experimental assembly.	23
Figure 3.1. Water Temperature input signal.....	27
Figure 3.2. Water temperature input signal (steady state period).....	28
Figure 3.3. Standard globe temperature response.....	29
Figure 3.4. Air temperature response (using Swema's anemometer).....	29
Figure 3.5. Comparison between measured air and operative temperatures.	30

Figure 3.6. Water temperature input signal (effective analysis).....	31
Figure 3.7. Air Temperature complete response (using Swema’s anemometer).....	32
Figure 3.8. Air temperature profile response (measured by the Thermistors).....	33
Figure 3.9. Standard globe temperature complete response.....	33
Figure 3.10. Globe temperature response (for miniglobes).....	34
Figure 3.11. Mean radiant temperature response.....	35
Figure 3.12. Plane radiant temperature response.....	35
Figure 3.13. Operative temperature complete response.....	36
Figure 3.14. Comparison between measured and calculated operative temperatures.....	36
Figure 3.15. Comparison between measured air and operative temperatures.....	37
Figure 4.1. Operative temperature behaviour approximation.....	40
Figure 4.2. Obtainment of the temperature difference.....	41
Figure 4.3. Heating power calculation table for the radiant ceiling panels.....	41
Figure 4.4. Equivalent model of the system.....	42
Figure 4.5. Thermal model approximation.....	44
Figure 4.6. PMV response (calculated by Fanger’s method).....	46
Figure 4.7. PMV response (calculated by Sherman’s method).....	49
Figure 4.8. PPD response.....	49
Figure 6.1. PMV scale.....	62
Figure 6.2. Metabolic rates table.....	64
Figure 6.3. Table of thermal insulation for typical combinations of garments.....	64
Figure 6.4. Representation of the AGS54 and AKF10 sensors.....	65
Figure 6.5. Air temperature transducer.....	66
Figure 6.6. MM0038 anemometer.....	66
Figure 6.7. Swema’s anemometer.....	67
Figure 6.8. Thermal comfort transducer.....	67
Figure 6.9. WBGT set of sensors (including the black globe).....	68
Figure 6.10. Thermokon’s miniglobe.....	69
Figure 6.11. MM0036 temperature asymmetry transducer.....	70
Figure 6.12. Thermistor calibration functions.....	71
Figure 6.13. Miniglobes calibration functions.....	72

NOMENCLATURE AND ACRONYMS

Nomenclature

A – Room surface area

$c_{p,\text{water}}$ – Specific heat at constant pressure of the water

c_v – Air specific heat at constant volume

D – Diameter of the globe

f_{cl} – Clothing surface area factor

f_{eff} – Ratio of radiating surface of the human body to its DuBois surface area

h_c – Convective heat transfer coefficient

h_{cg} – Convection coefficient at the level of the globe

h_r – Radiative heat transfer coefficient

I_{cl} – Clothing thermal insulation

k_q – Usage factor

M – Metabolic rate

m – Metabolism

\dot{m} – Air mass flow

m_a – Air mass

MRT – Mean radiant temperature

P – Net radiation

p_a – Water vapour partial pressure

Q – Heating power

$Q_{\text{boundaries}}$ – Balance of heat exchanges with the exterior

q_c – Convective heat exchange

$Q_{\text{infiltrations}}$ – Balance of heat exchanges by infiltrations

Q_{panels} – Balance of heat exchanges by the radiant panels

q_r – Radiant heat exchange

t – Time

- T – Generic temperature
- T_0 – Initial temperature
- T_a – Air temperature
- t_{cl} – Clothing surface temperature
- $T_{corr\ i}$ – Corrected air temperature measured by the i thermistor
- T_d – Dew-point temperature
- T_{ext} – External temperature
- T_g – Temperature of the black globe
- $T_{g\ corr\ i}$ – Corrected globe temperature measured by the i miniglobe
- $T_{g\ i}$ – Globe temperature measured by the i miniglobe
- $T_{g\ ref}$ – Reference globe temperature
- T_i – Air temperature measured by the i thermistor
- T_k – (k) Value of air temperature
- T_{k-1} – (k-1) Value of air temperature
- T_n – Net radiometer's temperature
- T_{op} – Operative temperature
- T_{prA} – Plane radiant temperature on side A
- T_{prB} – Plane radiant temperature on side B
- T_s – Skin temperature
- U – Global heat transfer coefficient
- V – Room volume
- v_a – Air velocity
- W – Effective mechanical power
- Y – Predicted mean vote (Sherman's method)
- Y_c – Convective comfort coefficient
- Y_e – Evaporative comfort coefficient
- Y_o – Basic comfort coefficient
- Y_r – Radiative comfort coefficient
- ΔT – Difference between the globe and the air temperatures
- ΔT_{power} – Temperature difference for power calculation
- Δt_{pr} – Radiant temperature asymmetry

ΔT_{water} – Water temperature difference between inlet and outlet

ε_g – Emissivity of the globe's surface

ε_s – Emissivity of the radiometer

λ – Infiltration rate

ρ – Air density

σ – Stefan-Boltzmann constant

τ – Time constant

Acronyms

HVAC – Heating, Ventilation and Air Conditioning

ASHRAE – American Society of Heating, Refrigerating and Air Conditioning Engineers

EAI – *Erythema ab igne*

CFD – Computational Fluid Dynamics

RHC – Radiant Heating and Cooling

RTD – Resistance Temperature Detector

PTC – Positive Temperature Coefficient

NTC – Negative Temperature Coefficient

WBGT – Wet Bulb Globe Temperature

PID – Proportional-integral-derivative

1. INTRODUCTION

Radiant heating is considered to be one of the most promissory, relatively recent applications of heating, ventilation and air conditioning (HVAC) and it has been developed both in industry and in research projects. In the present work it is intended to study this heating method and characterize an entire system, constituted by a large laboratory, the radiant panel circuit and, of course, the external context. In order to do that, the first main step is to get to know this technology.

1.1. State of the Art

1.1.1. Definition of Radiant Heating

As the words say, radiant heating consists in transferring heat from a source to an envelope or control volume exclusively by radiative process. Since human beings are so used to conduction and convection heating equipment, this heat transfer mode is slightly subjective to the majority of the people. Therefore it is important to establish the practical significance of this heating application.

The act of heating by radiation can be easily illustrated based on the most natural source of heat: the sun. The sun infra-red radiation heats the surfaces and bodies directly, instead of heating the air which, to a first approximation, is transparent to radiant heat transfer from hot bodies to cold ones. In the Figure 1.1, is represented an example of how the radiation influences beings.



Figure 1.1. Example of beings' behaviour when looking for thermal comfort.

In spite of having a lot of space on the floor, the cat decided to sit where he could receive sunlight, in order to feel warmer, even though the air is cold. This is observed in the cold seasons, and human beings also do the same to stay comfortable. Another technology used by people since the ancient times is the fire. The majority of the heat from a fire is received by radiant exchange.

Like what happens with sunlight, the radiation moves in straight lines, heating the surfaces it finds. By absorbing radiation, the bodies' temperature increases as an expression of internal energy rise by atomic and molecular excitation. Based on this principle, one advantage of this heating type is that it can be used directly to control the rate with which bodies loose heat, instead of doing it indirectly by rising the air energy like in convective processes.

In reality, the human perception of temperature is close to a weighing of the air temperature and the temperature of the surrounding surfaces combined. As an illustration, a room heated by a radiant ceiling is represented in the next picture (Figure 1.2).

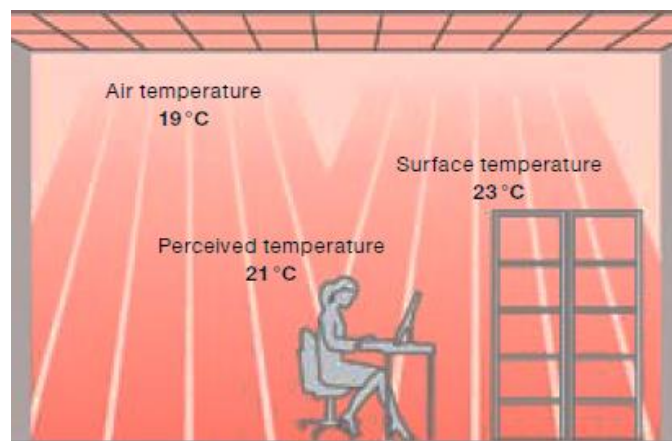


Figure 1.2. Perceived temperature with radiant heating.

Thanks to the radiant ceiling, the surfaces (furniture, walls, floor...) acquire a temperature of 23°C and, despite the air temperature being lower, the resulting perception is of thermal comfort.

As a consequence, the heat distribution up to the ceiling height is more uniform and there is not a significant variation from level to level. According to the document [1], this is much more effective than the typical vertical heat distributions for convective processes as it is seen in the Figure 1.3.

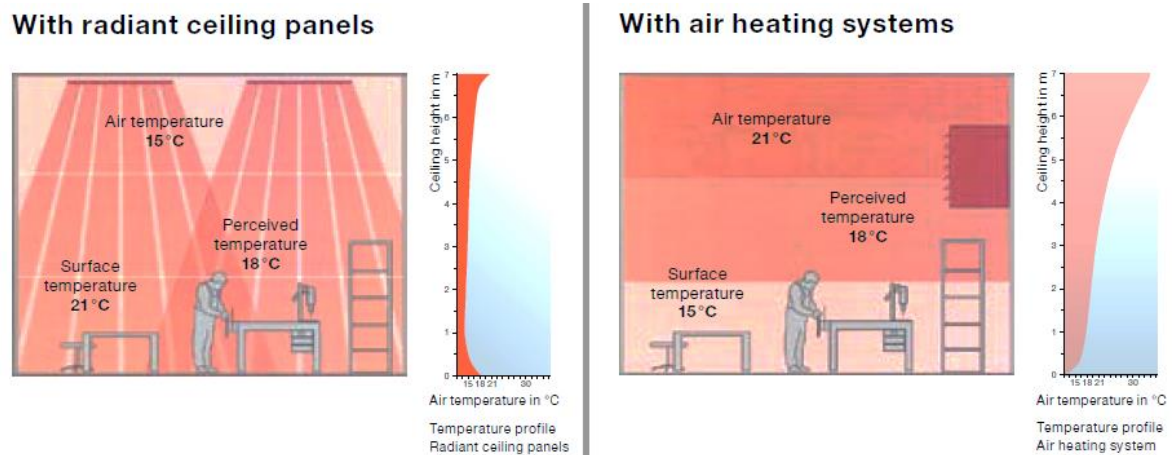


Figure 1.3. Comparison between radiant panels and air heating systems.

As it is possible to see, the perceived temperature is the same in both cases, the difference is that in the radiant heating case, the air temperature is 3 °C lower and in the air heating case, the air temperature is 3 °C higher. By consequence, and according to [1], using radiant heating the heat loss is significantly reduced and, therefore, there is a return in energy savings.

1.1.2. History and Context

Although radiant heating equipment is relatively new as a HVAC solution, this heat transfer process has been utilized for centuries or even thousands of years. In the Roman Empire, there were built air circuits (the Hypocausts) beneath the floors of buildings (public bath buildings mainly). Basically, the floor stood over pillars (like the ones represented in the Figure 1.4) and through the space between the pillars the hot air and smoke from the furnaces passed until the opened-sky flues, heating the floors of the rooms without polluting the interior [2].



Figure 1.4. Roman hypocaust.

The same principle was also applied in the Chinese civilization, where the smoke from the fireplaces was forced to pass underneath the house floors. In this case it was already being applied on residential buildings. It turns out that this technology was getting developed in Asia until nowadays, whereas in Europe it vanished for centuries until being restarted in the 19th century [3].

Nowadays it has been utilized in the shape of panels, ceilings and walls, mostly in the northern European countries, where the climate is colder and heating the air to comfort temperatures is expensive. In countries like Germany, Poland and United Kingdom, radiant panels have been a growing heating and cooling solution, both in office buildings and in sports pavilions. In the following figure (Figure 1.5) there are represented the examples of the Adidas Global IT Center (using flat ceiling panels) and the Sports Forum, both in Germany.



Figure 1.5. Examples of buildings with radiant ceiling panels.

The number of large buildings that are adopting these solutions is increasing since the energy certificate is gaining more importance and is being mandatory in some regions. Today, this consists in a great technology to include on net-zero buildings.

Both examples are related to models of the brand Zehnder, but there also other brands like Frengerwarm or Solray which produce not only water driven radiant panels but also electricity driven radiant panels. The brand logos are represented in the Figure 1.6.



Figure 1.6. Brands of radiant heating equipment.

The referred equipment examples are also following represented (Figure 1.7).



Figure 1.7. Types of radiant heating equipment.

1.1.3. Radiant Panels

Focusing just on radiant ceiling panels, which are the ones to be studied in the present work, these devices can be water driven or electricity driven. As both cases are very similar, this text will be centred in the water driven panels. The heating fluid (the water heated by a boiler, in this case) is circulated through insulated metal panels. The energy from the water is, as said before, transferred to the space by photons. By curiosity, based on this principle, the radiant panels are the only devices that could work in the vacuum. The radiant panels can operate, for heating, between 30 to 150 degrees Celsius, of course is just a matter of establishing the project heat load, depending on the room size, the initial temperatures, the exterior conditions and, of course, the required temperature for thermal comfort.

In spite of being widely utilized for heating application, radiant panels also allow cooling, if the input water is cold. In this case the principle is still the same, but instead of emitting radiation, the panel absorbs it. Also, instead of being supplied by a boiler, the water could be supplied by a chiller.

As a brief description of the radiant ceiling panels, they are commonly a system of tubes covered by a sheet metal plate (usually made of steel) connected to water collectors, and a layer of insulation in fibreglass for example.

In order to get to the present designs, many attempts and studies were made. The first reference to a radiant heating panel apparatus is from 1978, although radiant exchanges of heat have been studied since 1965, as it can be seen on the patent on [4].

This patent from Ohio (United States of America) corresponds to the first concept of a radiant panel as a “radiating or absorbing heat exchange panel”. The invention patent claims to innovate at the design of the heat exchanger, consisting of a sheet of aluminium

having assembled to it a copper tubular member with a non-circular section. The principle of work is the same, in the case of heated water circulation, the heat is transferred from the tube to the plate, raising its temperature in order to make it emit radiation. In the case of the chilled water, the energy is absorbed by the plate. In spite of being an early and rudimentary design, the considered materials were thought to have high thermal conductivity, but the most important gap between that concept and modern panels is the emissivity, which was certainly an improvement, whether for heating, whether for cooling, because the bigger the emissivity value, the bigger the absorptivity also.

Later, in 1999, the manufacturer Zehnder released an European patent corresponding to a technology for reducing production costs [5]. The invention consists in a plate element with grooves to allocate the circuit tubes with the possibility to be suspended like radiant ceiling panels from nowadays. This invention changed the configuration of radiant panels allowing them to be adjusted to large rooms with a significant height and to reach a level of about 60 to 70 percent of transferred energy by radiation. The other 30 or 40 percent of energy are transferred by contact with the surrounding air, or by other words, by convection. Which is legitimate, since a heating equipment is only designated as radiant once it transfers at least 50% of the heat energy by radiation.

More recently, in 2009, it has been presented a new design of pre-built panel to include in final building construction phases in order to make easier and aesthetically pleasant the usage of surface radiant heating and cooling on floors, walls and ceilings. The invention can be seen in the US patent [6]. The invention consists in a honeycomb layer with rigid upper and lower covers. The upper cover board has a cut channel through it, in a pre-established pattern of assembly, to allocate the tubes of the circuit. To insert the tubes on the panel some pressure is required in order to fit them into the aluminium honeycomb. In order to make a circuit is only necessary to assembly several boards in a puzzle scheme. Mainly the recent advances are in the panel design. Today a radiant ceiling panel has the following represented design (Figure 1.8).

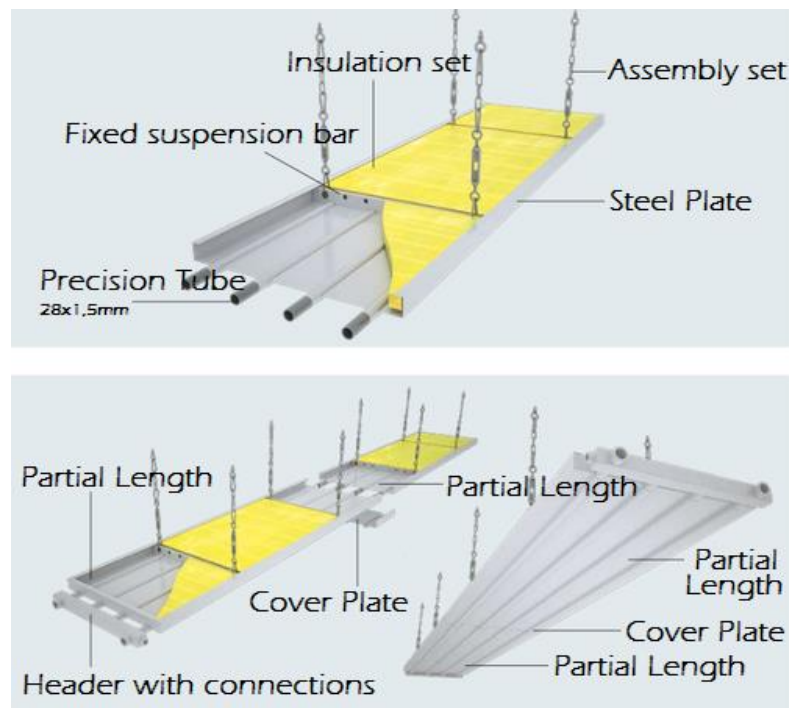


Figure 1.8. The radiant ceiling panel typical structure (Adapted from: Zehnder ZBN).

Today, shaped as they are, the usage of radiant ceiling panels result in several advantages. For example, there is a great improvement due to the fact that there is no forced air displacement. As result, there are no air draughts, which in the case of forced convection can be one cause of thermal discomfort. Besides, radiant heating doesn't significantly change the air humidity, therefore there is no need for humidification, the air doesn't become dry and that avoids the appearance of respiratory tract irritations or diseases. Another advantage is the cleanliness of the radiant heating operation, there isn't parallel production of smoke or dust, and heated surface attract less dirtiness than cold surfaces [7]. Mainly, radiant heating devices are safer, economic and more durable than other heating solutions. The initial and operation costs are lower than a hydronic heating system, for example.

In the United States of America, there was done an experiment by the American Society of Heating, Refrigerating and Air-Conditioning Engineers (ASHRAE), which consisted on installing several heating equipment corresponding to the available market solutions. Then a group of people was invited to be exposed to the different types of heating and asked to classify with a number. The results showed that, when exposed to radiant heating, people selected temperature levels, on average, 5 to 6 °C lower than any other heating method. And, experiments show that, in order to reach thermal comfort,

increasing the mean radiant temperature is more effective than increasing the air temperature.

But still, when people talk about radiation there are some doubts about the regular and widespread use of radiant heating. Frequently, manufacturers sell this solution as the most reliable even in the health factor. For the current case, radiant panels are said to be the healthiest heating device since they are appropriate for people with asthma, arthritis or allergies. Plus, this system has been also applied in maternity incubators [8]. However, people feel suspicious when hearing the word “radiation”. In fact, radiation produced by radiant heating devices is very different from sun radiation. Once the temperature of the objects is the parameter that defines the wavelength of the emitted radiation, both types of radiation encounter themselves on different spots on the electromagnetic spectrum. The hotter the body the higher the transfer of shortwave radiation. Radiant ceiling panels, being at a low temperature, emit longwave infrared radiation which doesn’t penetrate the skin surface. However, long exposures to this infrared wavelengths can lead to a skin condition called *Erythema ab igne* (EAI), in case of the temperature of the radiant surface being superior to 100 °C.

EAI, also called “toasted skin syndrome”, is a condition caused by long and repeated exposure to a heat source, creating patches on the skin that can become permanent and, in the worst cases, cause skin cancer. Figure 1.9 represents an example of a patient with this condition, a 22 year old young woman.

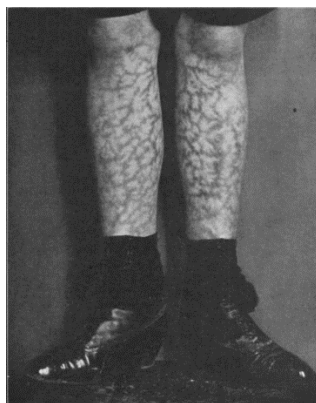


Figure 1.9. EAI skin disease symptom (Source: “*Diseases of the Skin*”, James H. Sequeira, 1915).

In order to clarify this health issues, some studies have been made, like the one which is presented on [9]. This study reveals, that after a long exposure to the heating source, longwave infrared radiation causes premature skin aging, like what happens with

UV light and, most importantly, “increases new, leaky vessel formation and induces inflammatory cellular infiltration”.

Of course this seems alarming but don't forget these phenomena happen for higher temperatures than the ones of the normal operation of radiant ceiling panels. Once again, radiation from ceiling panels is much different from radiation from hotter sources like the sun or even fireplaces. At least, until the moment, there wasn't any related health problem to do with radiant ceiling panels' usage and radiant heating is still considered very safe [8].

1.1.4. Studies on Radiant Panel Systems

Some works have been done in order to understand the behaviour of the indoor environment when heated by radiant ceiling panels. Figure 1.10 is an illustration of the number of radiant heating and cooling research projects for each part of the world.

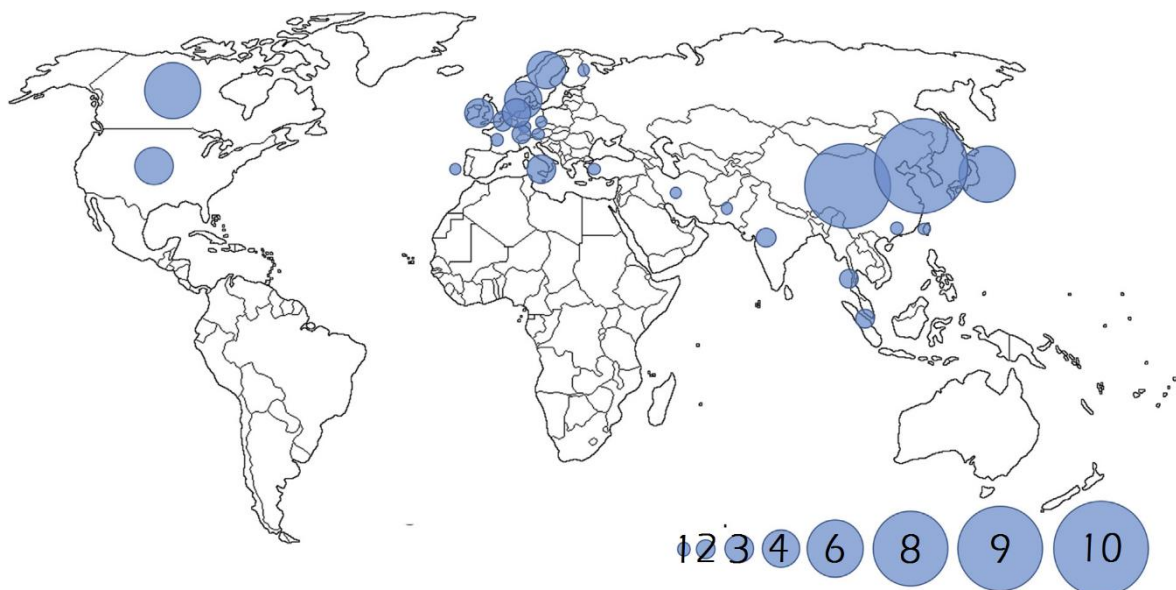


Figure 1.10. Location of radiant heating and cooling research projects.

In order to contextualize the reached developments in this area, there are following presented some examples of research projects.

In 1999, there was a research project about thermal comfort and energy consumption in an office building in Tokyo. In this article [10], the purpose of the study was to investigate the characteristics of radiant panel operation and their practical application to office buildings. There was made a comparison between a radiant ceiling panel system and an air-conditioning system in terms of thermal comfort, energy consumption and cost. The evaluation was made by the filling of questionnaires. The

results showed that the radiant ceiling panel system resulted in a small variation of air temperature and in a more comfortable environment. Concerning to the energy consumption and the costs, there was realized a numerical simulation of yearly energy consumption. As the volume of supplied air is reduced the energy consumption of radiant panels were lower by about 10% and depending on the market price and the usage, the radiant panel systems' predicted payback time was from 1 to 17 years. Besides these conclusions, the researchers always felt the notorious necessity for an “effective and less expensive control system of the ceiling panel temperature and room humidity (i.e., quick response to rapid change of the room condition)” and also for more reasonable costs of installation and bigger operation life.

The second example of research, held in Québec, is a 2012 article that presents a numerical optimization study of a heating ceiling and wall (water driven) radiant panel system in a residential building. The main variables analysed in the two dimensional computational fluid dynamics (2D CFD) program were the thermal comfort and the energy consumption. As these variables are contradictory objectives there was not obtained a unique solution but a set of optimal solutions (Pareto fronts). With the main design variables (the room geometry, the dimension of the panels and the inlet water temperature), the numeric analysis provided optimal solutions even though the total panel surface was reduced by 66%, which means the control of the inlet water temperature is the most important parameter to maximize thermal comfort on water driven radiant ceiling panels. Again, the control necessity is still put in a relevant position even 13 years after the previous referred article.

In the third article, [11] dated from 2014, the radiant panels were installed on walls, floor, and the ceiling of a reduced scale model room in order to investigate their performance. Temperatures of the room, including the walls temperatures, were experimentally measured. With the scaled room was also utilized a numerical model to study the flow pattern and predict the distribution of temperature. As result, it showed that this numerical technique could accurately predict temperature distribution in order to study the effect of the location and size of the panels and also the air flow and temperature distributions. It was concluded that the minimum transfer rates were achieved by heating panels placed on the floor which means that it is more productive to place them on the

walls or ceiling. And, besides that, the scale room model was capable of representing the real one with an error of about 20%.

The last article [12] is from the present year (2015) and contains a 50 year review on the researching of radiant heating and cooling systems (RHC). This study consists in a literature review to acquire a notion of the RHC researching trend. The review includes several approaches to the theme as in terms of “thermal comfort, thermal analysis including heat transfer model, heating/cooling capacity, CFD analysis, energy simulation, system configuration and control strategies”. The main conclusion is that RHC systems have been developed and are getting better in terms of thermal comfort and energy efficiency. As result, based on the review, there were suggested some topics for further studies. Among them, there are referred the following ones:

- System design and control for the RHC system that serves both heating and cooling;
- Integrated control of the RHC system and the building envelope (e.g. automated shade for reducing solar gain, and operable window associated with condensation control);
- Practical and simplified sensing technology of radiant temperature;
- Optimization of hydronic network system in terms of pressure and pumping energy.

Once again, the work developed until the present invokes the need for a precise monitoring and control algorithm for the radiant ceiling panel circuits, in order to establish the thermal comfort in a fast response to the external and internal conditions of the envelope climate.

1.2. Objectives and Motivation

Several previous works on radiant ceiling panels have raised the necessity for a consistent monitoring and control algorithm, capable of exploring the full capacity of this equipment, in order to turn them into highly efficient HVAC devices and transforming radiant heating in the 21st century indoor thermal comfort provider. Therefore the main objective of this work is to gain knowledge, from engineering first principles, about the way the radiant panels interact with the indoor climate and the perception of thermal

comfort. The objective is to identify and quantify the parameters that govern the interaction of the panels and their surrounding environment, to be able to characterise the whole system through a simple mathematical model. This is a first step that may be useful, in the future, for the simulation of control strategies and the development of an efficient control algorithm.

Figure 1.11 presents a schematised drawing of the radiant panels circuit studied in this work. There is installed a motorised bypass valve that can close the panels' circuit and a pump for recirculation, but at the moment the valve is fully open and the pump is always off because of the lack of the control system. In this specific case one of the potential application of the present work is the implementation of the identified physical parameters on a control algorithm capable of enabling the bypass in order to recirculate the hot water in the closed internal circuit of the panels.

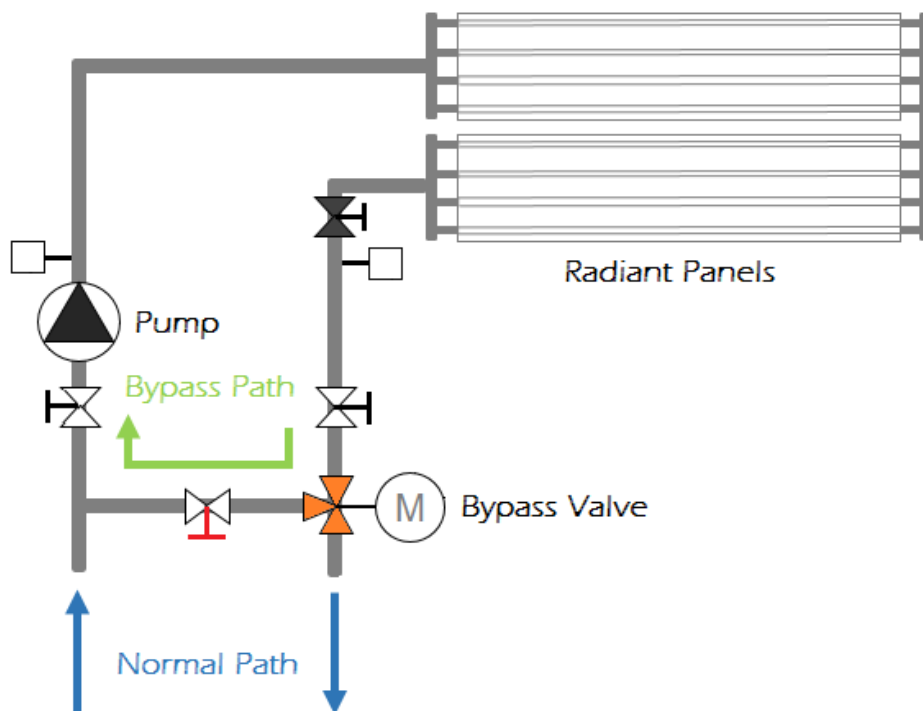


Figure 1.11. Simplified scheme of the radiant panel circuit.

The controlled bypass would result in a more efficient process once the heated water would not have to return to the boilers so often. The picture represents the flow in normal closed circuit operation, and then, the flow after bypass.

Of course, one of the motivations of this work is that the present experiment responds to the need for a simple thermal model that can be used in several other contexts serving as background for future monitoring and control approaches.

Not only is going to be studied the whole system, but as well, is going to be followed an approach to practical and simplified sensing of operative temperature and predicted mean vote for the radiant panel controlling. Remember from the section (1.1) that practical sensing is a fundamental need in controlling radiant ceiling panel systems.

Finally in order to acquire the notion of the elaborated research work it is presented in the following scheme (Figure 1.12), an inter-connection between the various approaches followed in this thesis.

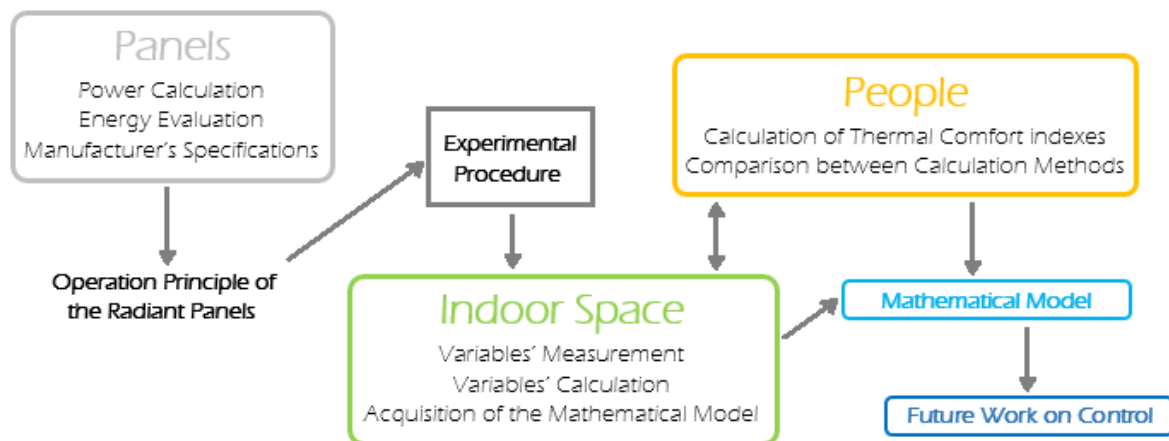


Figure 1.12. Scheme of the developed thesis work.

1.3. The Existing Radiant Panels Installation

The first step to define the behaviour of the variables previously referred is to make the experimental assembly in the radiant panel surroundings, in this case the laboratory. For that reason, it is shown, in this section, the resources and steps to complete the assembly.

In order to fully identify the studied system, it is important to start with its context. Concerning the building construction itself, the laboratory consists in a large room with a high ceiling (about 6 meters). The total volume of the laboratory is about 710 m^3 and its total surface area is close to 515 m^2 . The configuration and location of the contents in the room is represented Figure 1.13.

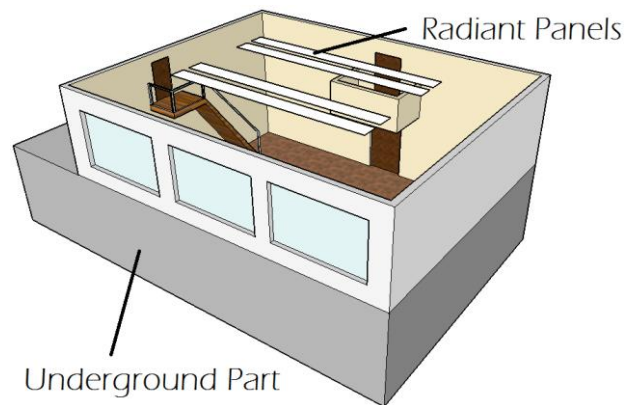


Figure 1.13. Model of the laboratory of the experimental activity.

The heart of the heating system is a pair of radiant panels mounted on the ceiling. This set of panels corresponds to the model ZIP2 from Zehnder, and has four long pipes properly isolated, disposed along the ceiling length. Their location can be checked in the Figure 1.14.



Figure 1.14. The radiant ceiling panel circuit of the experimental activity.

The two pairs of radiant panels from Zehnder are mounted on the ceiling and each one as a width of 70,4 centimetres and a length of 8 meters. The Zehnder ZIP2 dimensions are presented in annex A. A closer view of the radiant panels is presented in the Figure 1.15.

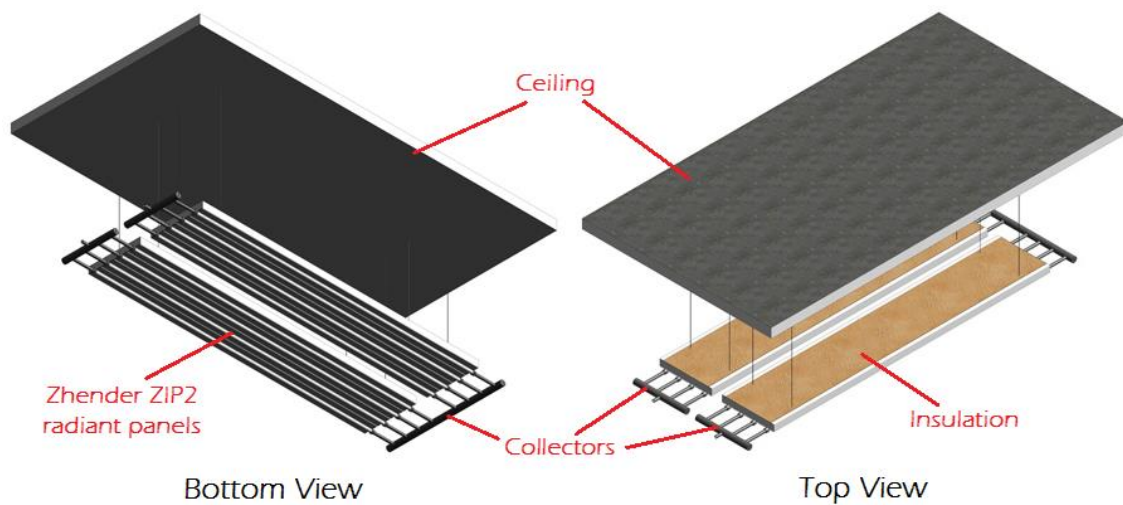


Figure 1.15. Structure of the Zehnder ZIP2 panels.

The panel material and the varnish white coat of paint is properly thought to have a high value of emissivity, around 0,79 [13].

Concerning to the operation condition, the whole system is set in a circuit that starts in the natural gas boilers. The closed circuit of the panels as 2 ways, the inlet and the outlet. The Figure 1.16 represents the circuit with the water track correspondent to only one pair of panels.

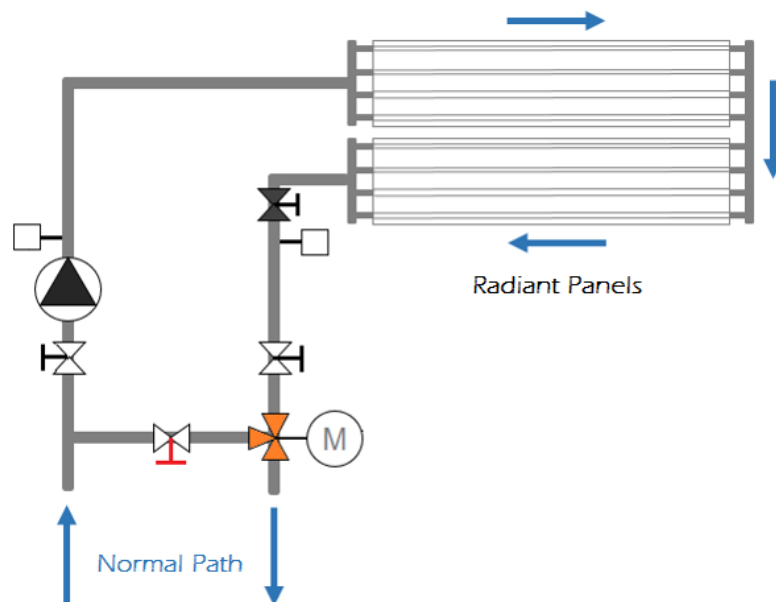


Figure 1.16. Water track on simplified opened circuit.

When the inlet tube valve is opened, the water, previously heated, enters, at more than seventy degrees Celsius, to the system providing a step input of energy. The same step

type signal is caused when the valve is closed, making the temperature return to the ambient reference.

The panels' water circuit is fed by a supply of heated water from the boilers of the department. The closed circuit of the radiant panels is internal (relative exclusively to the laboratory) and it has a pump responsible for taking the water into the panels, which is represented in Figure 1.17.

Also, this pump, placed in the inlet pipe, allows the water to recirculate in the closed panel system, when it is able to make the bypass with enough energy to supply to the laboratory environment, and that, as shown before in this document, is the main objective to achieve. This pump from Wilo is indicated to work with water at a temperature of up to 110°C.

In addition to this pump, the circuit has other important components: the balancing valves and the bypass valve. The second one is possible to see in the Figure 1.17, where it is represented the zone of the bypass of the internal radiant panel circuit.



Figure 1.17. Bypass zone of the circuit.

Noting the pipes have a diameter of $\frac{3}{4}$ of an inch and are properly isolated to maintain the water temperature and, of course, to avoid significant heat transfer by conduction and convection through the pipes to the environment. As well as is important to note that the white boxes in the figure contain water temperature sensors whose characteristics are going to be referred later in this document, in the Appendix B.

The bypass ball valve has a modulating rotary actuator that, as its name indicates, actuates a distributor electrovalve and is the orange device represented in the figure above.

1.4. Operation of the Existing Radiant Panels

To control the operation of the radiant panels, it is necessary to monitor thermal comfort parameters, such as the air temperature, the operative temperature, the exterior temperature, the air velocity and the mean radiant temperature, of course. Mathematically, those variables obey to a typical response of a first order system. That means, the time evolution of the variables behaviour can be well described by first order differential equations.

In this case, the input to the control system is represented by the temperature of the hot water. Now, at this point, it is assumed that the water is already heated by the boilers and circulating along the whole building circuit. For that reason, when switching on the flow into the panel's circuit we are causing an abrupt signal input. Which results in a natural exponential response, as seen in the Figure 1.18.

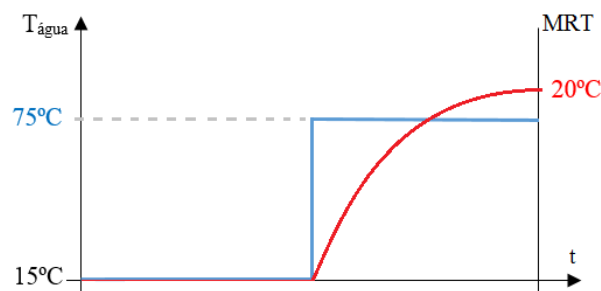


Figure 1.18. First order response.

The internal environment takes a while to acquire a certain fixed value of mean radiant temperature, showing a typical delay due to the natural system inertia. Focusing on the controlling process of the panels to be developed in future work, every time an input of the same type occurs, the whole system has the same mathematical response behaviour:

$$\frac{T(t) - T_{eq}}{T_0 - T_{eq}} = e^{-\tau t} \quad (1.1)$$

Where:

T – generic temperature, in kelvin (K)

T_0 – initial temperature, in kelvin (K)

τ – time constant, dimensionless

The present work is going to approach the thermal behaviour of the system to a model based on this type of response.

With an obtained thermal model of the system, if it is known the period of time that the MRT exponentially takes to get to a certain comfortable level, for example, it is possible to set the signal input (hot water intake) for a precise instant that ensures the maintenance of the temperature between two pre-established limit values (considering a confidence interval around an ideal value of temperature), as illustrated on the Figure 1.19.

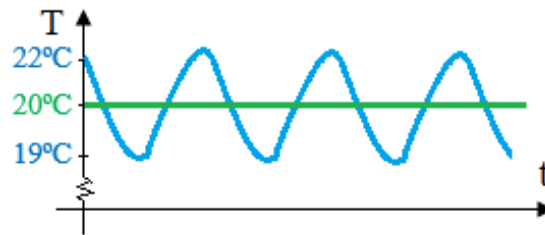


Figure 1.19. Example of the input actuation for a set of a certain output value.

This behaviour is inherent to the majority of the measured variables in the system.

2. MATERIALS AND METHODS

2.1. Experimental Assembly

The experiment work developed for this thesis occurred during a sunny winter, corresponding to the months of February and March, in which the average temperature was about 14 degrees, far away from the typical severe conditions of a winter in the northern countries of Europe, where this type of heating system is usually applied.

2.1.1. Introduction to System Identification

The system identification is an intervention that provides the mathematical or physical description of a dynamic system and the algorithms which allow the construction of representative models.

To identify a system is necessary to complete three tasks:

- The measurement of the input variables which affect the system;
- The measurement of the output variables which characterize the response;
- Finding a mathematical correspondence between the inputs and the outputs.

These stages correspond to the main frame of this work, which also includes the main considerations and discussions about the operation of the system. In the present case, it was opted to proceed on a simple method apart of the computerized model approaches presented on nowadays scientific studies on radiant panels' systems, and the following sub-section (Section 2.1.2) starts to define the inputs and the outputs to analyse.

2.1.2. Instrumentation

In terms of inputs to the radiant panels – laboratory – occupants system it is necessary to consider two variables: the exterior temperature and the panels' water temperature, as illustrated in the Figure 2.1.

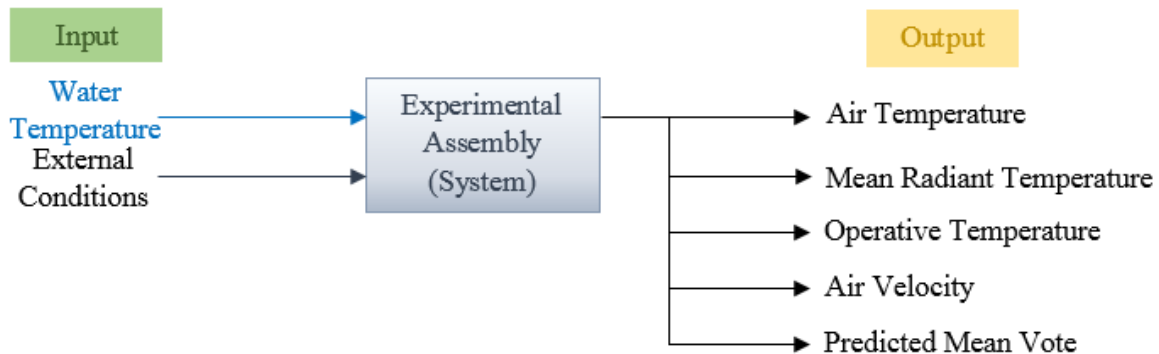


Figure 2.1. Experimental assembly objective scheme.

The external conditions are represented by the exterior temperature which was measured by the model AGS54, from Thermokon temperature sensors, which is resistance temperature detector (RTD) device, in this case, with a platinum 1000 ohms resistance (a PT1000).

Regarding to the other input, the water temperature, this one is measured in both routes of the radiant panel circuit, the inlet and the outlet. The temperature sensor which is in charge of that task is the Thermokon AKF10 that, as the previous one, is also an RTD PT1000. These sensors are very similar and are presented in the Figure 0.4, Appendix B.

Now, focusing on the outputs of the whole system, there are two indoor climate analyzer modules from Bruel & Kjaer (BK modules) and a DAQ (Data Acquisition) module from National Instruments connected to a computer. One of the BK modules, the type 1213, was connected to the reference dry bulb air temperature sensor, an anemometer and the thermal comfort transducer. These devices are described in the Appendix B.

The other module, the BK 1219, was connected to wet bulb globe temperature (WBGT) set, in which was present a standard black globe to measure the radiant temperature through the globe temperature. This BK module was also connected to a plane radiant temperature transducer in order to measure the difference in radiation between the floor and the ceiling. Both sensors are also described in the Appendix B.

The DAQ board was connected to the exterior and water temperatures sensors, but were, as well, connected to a couple of little black globes from Thermokon and a Swema's anemometer. The black globes were utilized in the experiment in order to try to validate its usage on a practical monitoring and control system, in order to calculate the mean radiant temperature. The anemometer was mounted as an additional air temperature and velocity transducer, once its response is faster than the anemometer from the BK1213. Once again, the descriptions of these sensors can be consulted at Appendix B.

Concerning to the air temperature measurement, it was utilized a thermistors bar with 5 sensor in a wireless network. Basically this bar has the main purpose to trace the vertical profile of air temperature by measuring this variable every 50 centimetres from the bottom sensor which is placed 10 cm above the floor. In the Figure 2.2 is represented a thermistor attached to the bar.

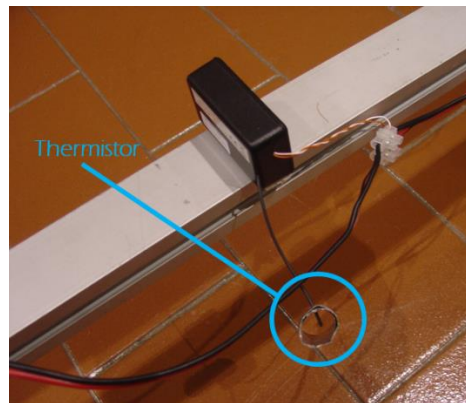


Figure 2.2. Wireless thermistor.

Following this step, the five available thermistors were mounted on a 2,5 meter bar to place on the vertical, in the experimental local. The wireless sensors were spaced 0,5 m, and the first thermistor was placed 10 centimeters from the floor, as already referred in the previous section. The vertical thermistor bar is represented in the Figure 2.3.



Figure 2.3. Thermistor vertical bar.

Then, some shield tubes were made from aluminium foil to protect the thermistors from radiant exchanges with the surroundings, in order to determine the most reliable values of air temperature, as seen below, in the Figure 2.4.



Figure 2.4. Thermistor with aluminium foil protection.

After everything connected, and the set of sensors placed in a proper scaffold structure, the instrumentation is placed in the proper place, in the middle of the room and near to a work zone, with the indicated configuration in the picture. To ensure that the measurements were the most reliable, the sensors were placed at the abdomen level of a

person seated in the laboratory, and all precautions were taken to not interfere with the sensor surroundings. The complete instrumentation set can be visualized in the Figure 2.5.



Figure 2.5. Experimental assembly.

2.1.3. Data Acquisition

In order to work with the instrumentation set beyond the analyser modules, it was necessary to proceed with the assembly and installation of the necessary structures and equipment to acquire the required data, already referred to in the previous section of this work, to properly identify the present first order system.

First, it was installed an acquisition board (also called DAQ boards) in the experimental activity's computer (the model SCC-68 connected to the PCI-6220 from National Instruments).

After the assembly of the boards, the two little back globes and the water temperature sensors from Thermokon where connected to the only signal conditioner utilized on the data acquisition, the SC-RTD01, also from National Instruments.

Next, the BK1219 module, corresponding to the WBGT index measurement, was also connected to the DAQ board with the SwemaAir 300 anemometer.

All the modules were connected to the computer and to visualize the output signals from all the sensors a computer program was created, in LabView, which is shown in the Annex B at the end of this document.

2.1.4. Calibrations and Adjustments

The first necessary calibration was executed on the five thermistor bar, which was placed in the horizontal with the purpose of getting all the sensors at the same level. During 23 hours, the wireless thermistors sent data to the computer and as it was expected, the curves of the air temperature of the five thermistors approached to a more restricted range. However, there was a difference from sensor to sensor. This temperature difference is inherent to each sensor in comparison to a reference thermistor which, in this case is the number 3 (the middle thermistor) because it is closer to the level of a seated person while the bar is in the vertical. When the sensors measure the same values of temperature, the function that relates the temperature measured by the reference sensor (thermistor number 3) with the temperature measured by the sensor to relate corresponds to a straight line that passes through the origin and as slope of 1. Therefore there were made four graphics, one for each relation (T_1 with T_3 ; T_2 with T_3 ; T_4 with T_3 and T_5 with T_3), represented in the Figure 0.12 on the Appendix C, knowing that there are already represented the trend lines obtain with the minimum square method.

After this, in order to make the y equal to the x (Temperature 1 equal to Temperature 3, for example), having the relations of the temperatures defined in a $y = ax + b$ equation, the properly said process of calibration consisted on subtracting the b value to the y (temperature to relate) and then divide the result by the slope m . After the application of these correction factors in the calculus sheet with the data from the wireless sensor network, with the thermistor bar in the horizontal, the sensors measured identic values.

Based on the same calibration method, it was necessary to calibrate the little black globes from Thermokon. After a short period of data acquisition, it was noted a difference of about 1 to 2 degrees of the measured globe temperature, comparing with the standard globe. Once again, the objective is to allow the three black globes to measure similar

values and, when that happens, the function that relates the miniglobes temperature with the temperature of the standard black globe consists to a straight line that passes through the origin and as slope of 1. Following this line of thought there were plotted two graphics (presented in the Appendix C), one for each Thermokon globe to compare with the reference values, and obtained the two trend lines. Like the previous calibration procedure for the thermistors, it is necessary that the y value turns equal to the x value in order to have the equality condition, and for that is a question of subtracting the origin y value and divide the result by the slope. As result the miniglobes are then able to acquire similar values for the same level/height with the applied calibration factors that can be seen in the Appendix C.

2.1.5. Measurement Procedure and Calculation of Derived Quantities

After the positioning of the whole instrumentation set, it started to acquire data during two campaigns. In the first one it was purposely turned on the radiant panel circuit for a short period and in the second, the system was evaluated during a long period in which the radiant panels' circuit were switched on alternately and the external climate changed with the season changing from winter to spring.

Then, all the values were logged, labelled, data stamped and then imported to Excel calculus sheets to proceed on the results analysis. The first calculus sheet utilized corresponds to the short period of 19 hours when the panels were deliberately switched on, with the purpose to proceed with preliminary analysis, whose results are going to be presented in the Section 3.1 of this work, in order to infer of the quality of the registry, of typical behaviours and variables response, for example.

The effective analysis consisted in the analysis of the final set of values already obtained by the experimental measures. Since part of the results still had to be calculated from the gross data, there were required some procedures to obtain the final results.

It was calculated the medium radiant temperature and the operative temperature utilizing the formulas presented on the Appendix A. These values were calculated for each black globe, since the MRT depends on each globe temperature, as well as the operative temperature depends on each MRT calculated value.

Besides this temperatures, it was also calculated the PMV index. The first difficulty was, once again, the data size, since the Fanger model [17] stands requires an iterative calculation. The need for searching for a non-iterative method lead to a simplified approximation of PMV calculation proposed by Sherman [18]. Once again, there was calculated a value of PMV for each MRT value correspondent to the each one of the black globes.

Lastly, the final results of the referred procedures can be observed in the Section 3.2.

3. RESULTS AND DISCUSSION

3.1. Preliminary Analysis

In the Section 2.1.4, there was referred that there was a first run of the radiant panels' circuit to infer of the quality of the data acquisition and typical behaviours of the system. Those 19 hours of first running are then represented in this section for all the measured data.

Well, the first thing to evaluate is the input signal, by other words the water temperature, whose data is represented below (Figure 3.1).

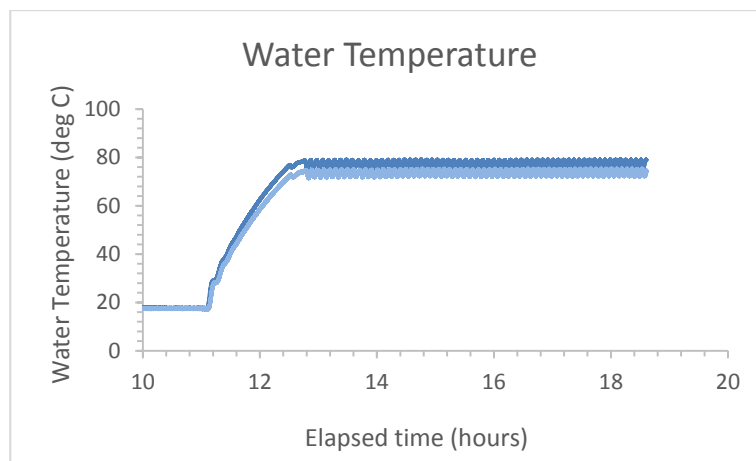


Figure 3.1. Water Temperature input signal.

The first characteristic that defines a first order system, as said on the section (1.4), is the step shaped input signal as it was expected in this case. However, when the circuit is connected (more or less at the point of 11 elapsed hours), the water temperature doesn't acquire the maximum level suddenly, it actually grows exponentially, taking about one hour and ten minutes to reach the temperature of operation. The only found reason for this is that, in the moment when the circuit is opened, the water from the boiler still isn't warm once the boilers just switch on in the morning. By other words, when the water starts to flow through the radiant panels' circuit, it has still to be heated by the boilers and that process occurs along the water input in the circuit. In result, the step isn't perfect once the increasing phase has an exponential behaviour. Just in the final results, during the effective analysis, is going to be possible to infer of the approximation of the signal to an input step.

The next particularity of the input signal is only detected with a single part visualization. The next graphic shows, on Figure 3.2, the water temperature on the inlet (upper curve) and on the outlet (lower curve).

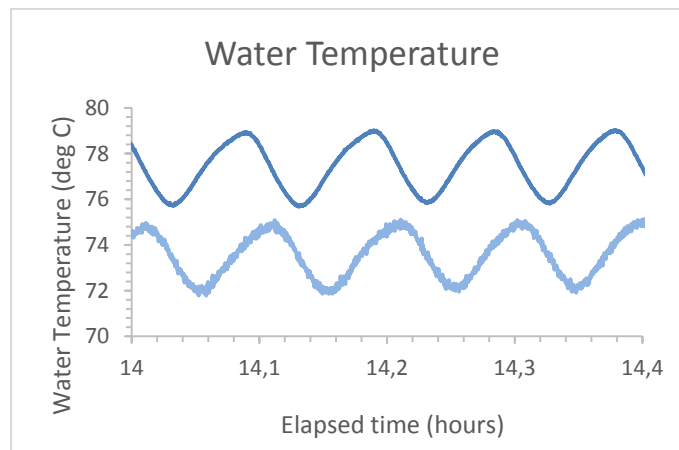


Figure 3.2.Water temperature input signal (steady state period)

What happens in this case is that the top values of temperature are not constant, their behaviour consist in a succession of exponential increases and decreases, which, after all, makes all sense, once that, in order to fix a maximum temperature to the water, the boilers have to activate and deactivate after a certain period in order to prevent overheating as well as overcooling and reaches values around that reference, once that physically is impossible to maintain the same temperature. By other words, the period of the signal corresponds to the period of the boilers actuation, which is about 6,1 minutes (about 0,1 hours) as it is possible to observe in the graphic.

Another conclusion that is possible to take from this graphic is that the difference between the two signals (the input and the output) is about 4 degrees, which means the water loses that same amount of temperature when releasing energy to the environment through the radiant panels. This is an important particularity once it allows the calculus of the total energy supplied to the indoor climate.

Another fact is that, as it is possible to see, there is a mismatch between the inlet and the outlet signals and this corresponds, precisely, to the time of water circulation in the complete panels' circuit. The value of this mismatch, graphically obtained, corresponds to almost 80 seconds.

In what concerns to the response, the standard globe temperature is then presented, in the Figure 3.3.

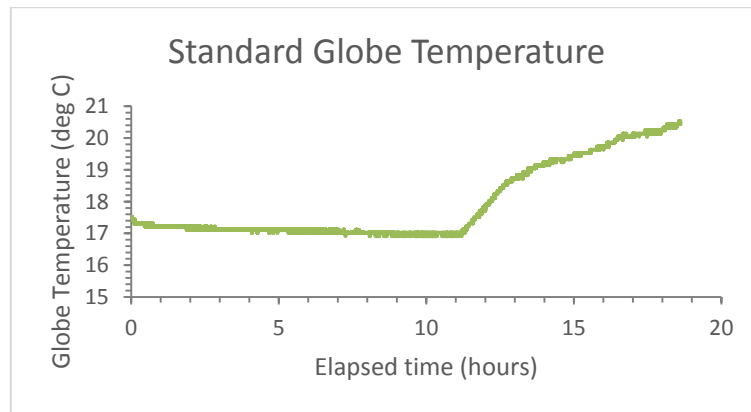


Figure 3.3. Standard globe temperature response.

What is possible to observe in this graphic is the exponential growth of the standard globe temperature in response to the input signal, however, there's a period of about one hour and ten minutes where the behaviour is almost linear. Of course this last referred period can be explained by the water temperature increasing period that goes from off to full operation, remembering, the signal input is not a perfect step.

Another important conclusion is that, for a loss of about 4 degrees in the water temperature, the standard globe temperature increases about 4 degrees too (from 17 to 21 degrees).

Next, the same behaviour is described by the air temperature. In the following graphic, Figure 3.4, it is represented the air temperature measured by the Swema omnidirectional sensor.

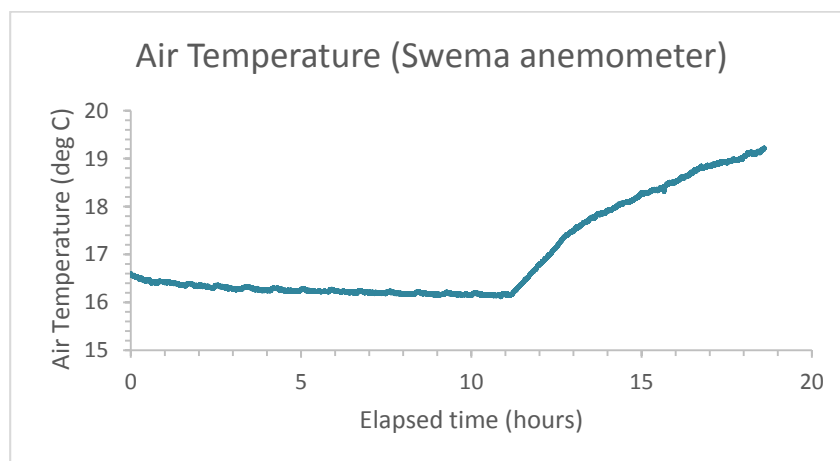


Figure 3.4. Air temperature response (using Swema's anemometer).

In this case there is a difference of about 3 degrees from the initial state to full operation. Still it corresponds to high value of heat input directly to the air. Although the surfaces heat up faster, the part of the total load that is being directly supplied to the air

seems to be too much. One way to know if that's appropriate or not is to calculate the PMV, if it acquires a value near to the warmer zone, it means that the radiant panels might be supplying too much energy to the room.

The air temperature was also measured by a reference air temperature sensor. In the following graphic, Figure 3.5, is represented the obtained values of that measurement and also of the operative temperature measured with the thermal comfort sensor.

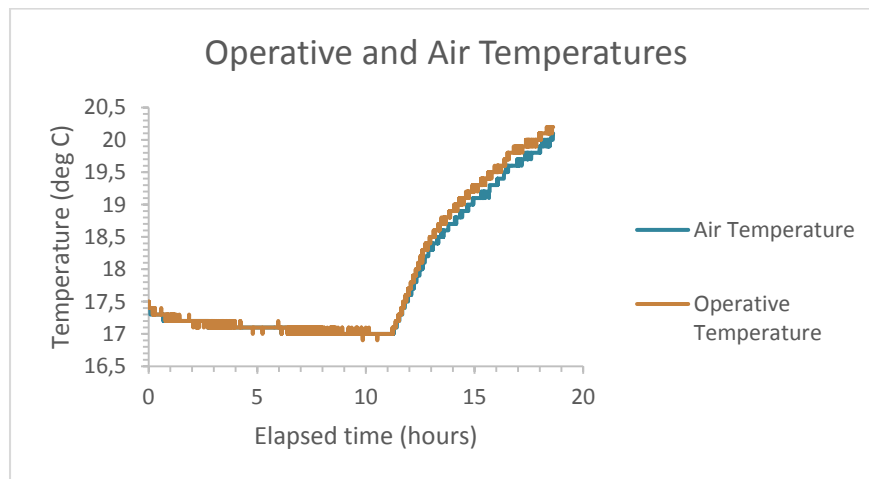


Figure 3.5. Comparison between measured air and operative temperatures.

In what concerns to the operative temperature there's nothing new except the fact it stands between the air temperature and the globe temperature values, which makes all the sense, since it is weighing of the medium radiant temperature (calculated with the globe one) and the air temperature.

The main particularity of this representation is that, both values are too close and this can be another signal that there might be introduced too much heat directly to the air of the room.

3.2. Effective Analysis

In this section of the present thesis, it is presented the acquired data from the experimental assembly referred in the Section 2.1.4.

The first data to analyse is the input signal of the system: the water temperature. As It was possible to see on the preliminary analysis, this variable had a slightly different behaviour from the step one, once the water on the boilers still had to heat up, the step as not as spontaneous as it would be expected. Remembering, the exposed data on the preliminary analysis didn't had the period of the water temperature decreasing, which

starts immediately after the switch off of the radiant panel circuit. By other way, the complete water temperature behaviour is represented in the following graphic, Figure 3.6.

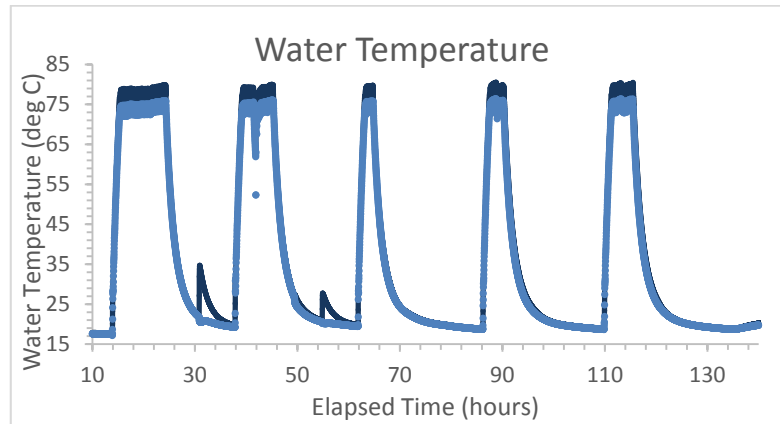


Figure 3.6. Water temperature input signal (effective analysis).

What is possible to observe in this picture, is that, in fact, there is a signal input behaviour very similar to a set of several steps. This is one of the main characteristics of first order systems as related in the Section 1.4. However, besides the exponential tendency of the water temperature on the switch on moment, also exists an exponential tendency, even more relevant, on the switch off moment. It sure means, that the temperature increase is more rapidly done than the temperature decrease to a minimum stable temperature. That only can significate that there is some water left in the panels several hours after the switch off and this behaviour is the result of the inertia of that same amount of water in its natural cooling process. Another supposition is that some amount of water might take a bit more time to flow out on the circuit, otherwise, it couldn't be observed so much hours to get the minimum temperature.

In order to maintain the line of thought of this work, as well as to validate the results, It is still valid the consideration of this input signal as a first order input, and, in fact, it causes a very well mathematically defined response, as it is possible to see through the next graphic Figure 3.7, for example.

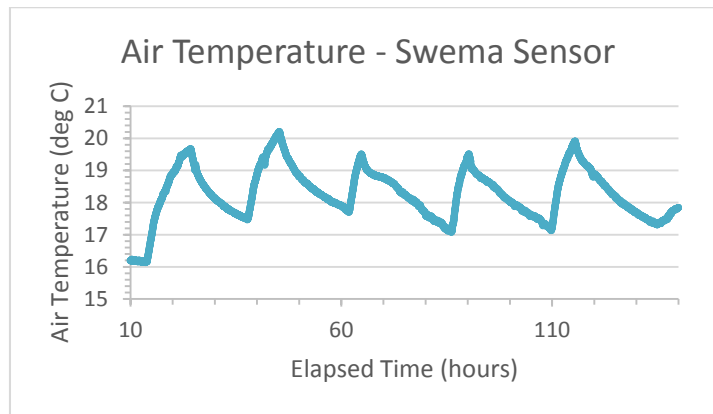


Figure 3.7. Air Temperature complete response (using Swema's anemometer).

The graphic above corresponds to values of air temperature measured by the Swema air velocity transducer which, as seen in its description in the Appendix B, is also capable of determining the air temperature.

The represented period (from 10 to 130 hours) consists in a five days sample, each one represented by one peak. Now, the main characteristic to retain from this behaviour is that in the first moment the room air temperature (dry bulb) is about 16°C, and that value isn't reached anymore during those five represented days. Once the radiant panels' circuit was switched on, it started a process of heat accumulation, from day to day. As it is possible to see, mainly in the first 3 peaks, is that each time the temperature starts to rise, it increases from a higher value of room temperature, and that happens due to the fact that the input energy from the previous day is still bigger than the total losses during the non-operation period. This accumulation process can also be explained, in part, by the possibility of the outside temperature increase, although it isn't very effective. The successive accumulation of energy might induce thermal comfort alteration and, for long continuous periods, can lead to energy inefficiency.

Still concerning to the air temperature, there's another characteristic to analyse, it's variation along the height of the room. The next graphic (Figure 3.8) shows the variation of the air temperature for different height values.

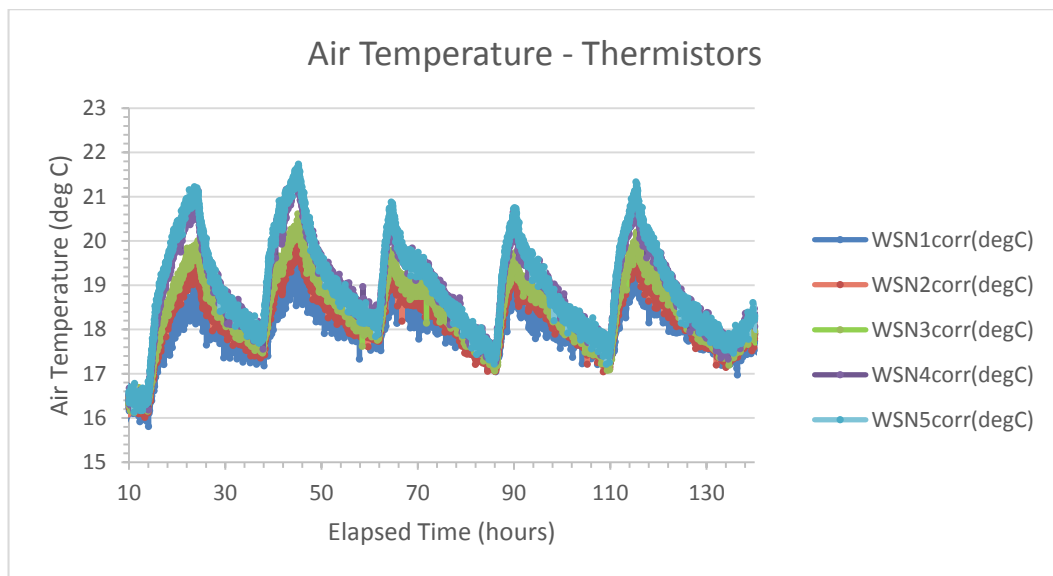


Figure 3.8. Air temperature profile response (measured by the Thermistors).

As said in the Section 2.1.1, to measure the temperature at different levels, it was used a vertical bar with five wireless connected thermistors. Placed in order, the WSN1 stands for the sensor 1 placed 10 cm above the ground, and the WSN 5 corresponds to the sensor on the top at a height of 2,10 meters. The main conclusion to acquire from this graphic is that the vertical distribution of the air temperature has just a slight variation which means the temperature is almost vertically uniform as a result of lower heat amount directly transferred to the air that defines the radiant heating devices.

Identical behaviours can be observed in the remaining variables. In the following graphic (Figure 3.9), there is represented the example of the standard globe temperature.

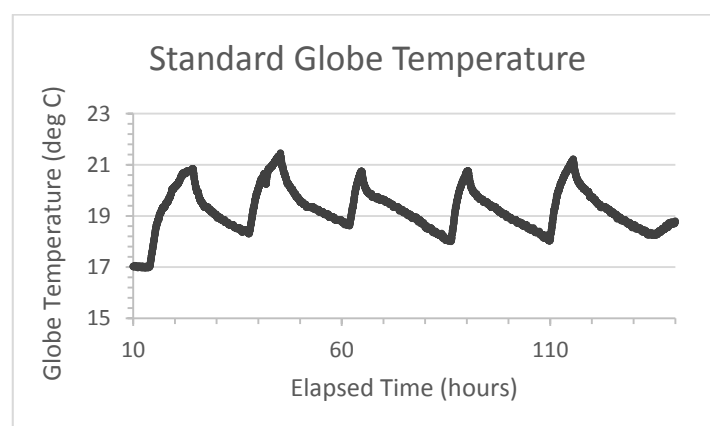


Figure 3.9. Standard globe temperature complete response.

The only important fact to retain is that these globe temperature values are higher than the air temperature values measured at the same level of the standard black globe

(more or less 1 meter), the normal level of a person seated in a laboratory. By other words, in order to compare the previous graphic with this black globe temperature evolution, is necessary only to considerate the WSN3 sensor (the one placed near the 1 meter level). Comparing both, it is noted a difference of more the 1 degree. Well, since the black globes have the main purpose of calculating the radiant temperature, it is normal, that, with a significant amount of radiation, it presents a higher value of temperature.

Next, there is a representation, on Figure 3.10, of the measurement of the globe temperature, recurring to the smallest globes.

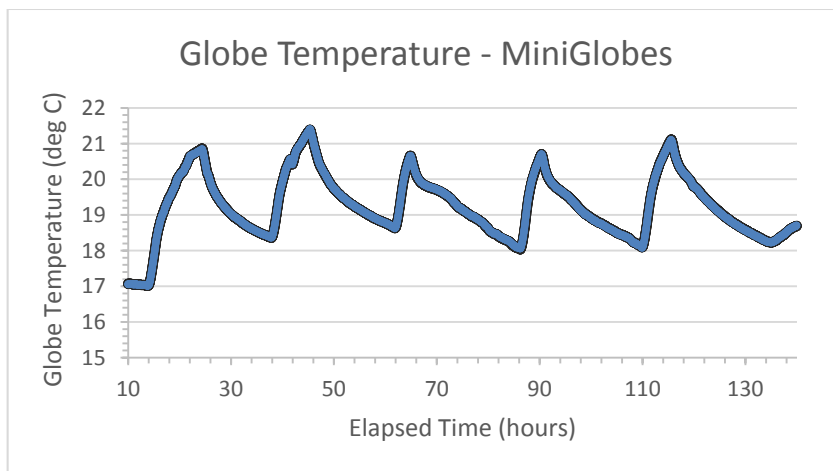


Figure 3.10. Globe temperature response (for miniglobes).

As it was expected, there's practically no difference between this values and the ones measured by the standard globe, and so the response is well defined. Which is great news, since the main objective of this measurement is to infer of the usability of the smallest globes in a hypothetical control system for the radiant panel circuit, therefore is completely legible, by observing the results, to use this sensors as a more convenient and practical sensor solution.

After getting to know the globe temperatures, the necessary data to calculate the medium radiant temperature became available. The MRT is perhaps the most reliable variable to note the radiant heat transfer in the system and is then expressed in function of the elapsed time in the following graphic (Figure 3.11).

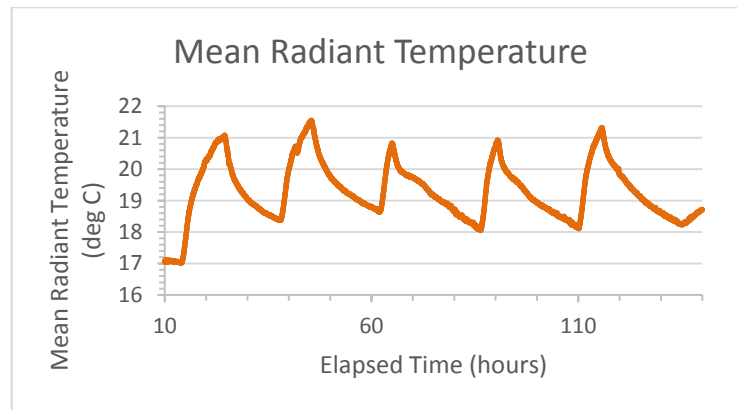


Figure 3.11. Mean radiant temperature response

As seen, the mean radiant temperature value is very similar to the black globe temperature, in spite of being different concepts. And, as it is pretended, the values of the medium radiant temperature are higher than the air temperature for the same level, simply due to the operation of the radiant panels.

Because the radiant heat transfer is not uniform in the whole space, it is also interesting to understand how are the surfaces emitting and reflecting radiation, as the ceiling and the floor. The variable which allows to infer of that is the medium plane radiant temperature. The next graphic (Figure 3.12) represents the plane radiant temperature along time, related to the ceiling (upper signal) and the floor (lower signal).

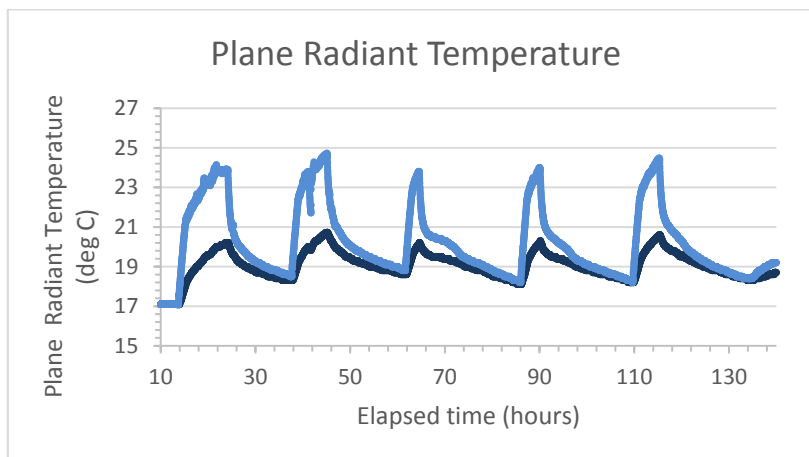


Figure 3.12. Plane radiant temperature response

By observing this graphic, the obtained difference between the ceiling (where the panels are mounted) and the floor is about 3,5 degrees which consists in a significant value, although reasonable, since the upper surface of the sensor is directly facing the radiant panels, while the other has a lower optic field of the ground.

What can be concluded is that the floor is actually reflecting a significant part of the received radiation from the panels, which, once again, causes the near air mass to heat up.

After calculating the medium radiant temperature is possible to calculate the temperature that best defines the real value felt by the occupants: the operative temperature, represented in the graphic below, Figure 3.13.

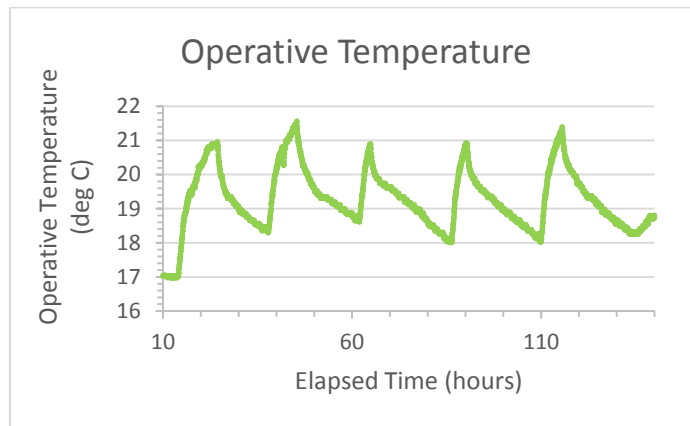


Figure 3.13. Operative temperature complete response.

By definition, being the weighing of the air and medium radiant temperatures, the operative temperature stands among both temperatures, and that's exactly what is observed in the picture, in spite, being close to the MRT values.

The comparison between the measured and the calculated operative temperature can be visualized in the following graphic (Figure 3.14).

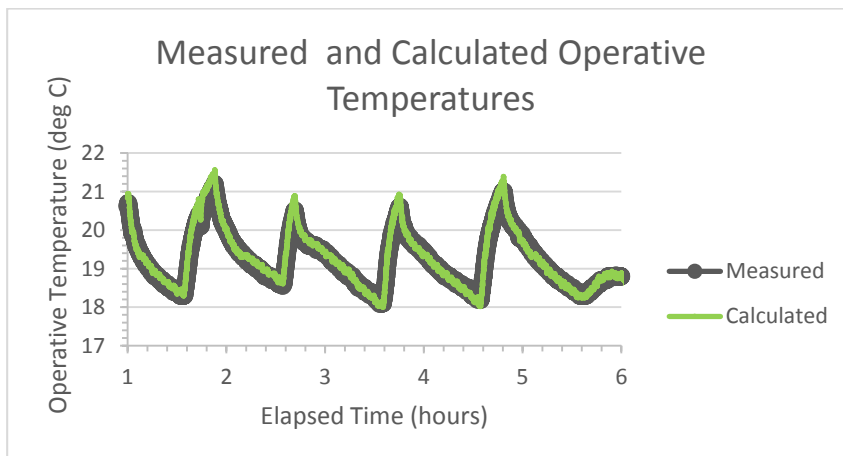


Figure 3.14. Comparison between measured and calculated operative temperatures.

Once both representations are very similar, it means that the operative temperature can be calculated instead of measured without precision loss, in a practical monitoring and control system.

With an idea of how close are the values of operative temperature from the values are from the medium radiant temperature, is now time to a comparison with the air temperature, as it is presented on the next graphic (Figure 3.15).

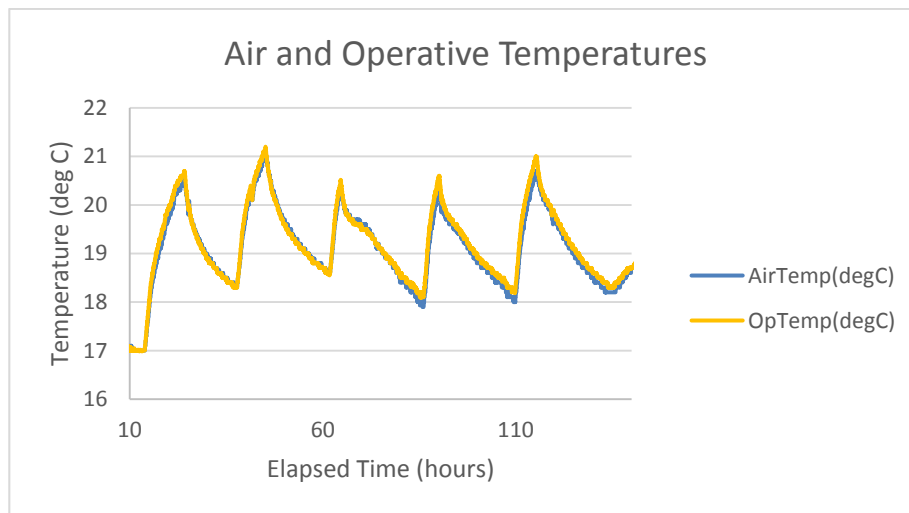


Figure 3.15. Comparison between measured air and operative temperatures.

It was expected a bigger disparity between the air and the operative temperatures. Basically, it is concluded that the radiant panels are transferring a substantial amount of heat directly to the air mass, although the majority of energy is obviously transferred by radiation.

4. SYSTEM IDENTIFICATION

In order to fully identify the system, it is necessary to acquire knowledge about the radiant panels (of course the core of the experimental work), the climate as an input through outdoor conditions and as an output through the natural behaviour of the indoor space variables and their response to the radiant panels operation, and, last but not least, the occupants conditions in order to enable the future control of the radiant panel circuit to be focused on the proper thermal comfort requirements.

4.1. Estimating the Power Output of the Radiant Panels

Concerning to the radiant panels, the main parameter that characterizes the whole equipment is its heating power. With this value it is, not only possible to acquire the notion of the total heat load in the indoor environment, but it is, as well, a means of comparison between this equipment and other present solutions on the market for the same heating needs. Therefore the first part of the data usage is then applied in the search for heating power value.

The presented heating power calculation method is related to the manufacturer's project calculus scheme, which consists on the normalized path to select a set of panels of a certain type for a determined heat loss suppression, and is based on the nominal heating power released for each meter of the radiant panels as well as the collectors that also transfer a relevant amount of heat to the space. The nominal values for the radiant panels and collectors are tabulated for each type of panel and depending on the temperature difference between the panels and the indoor space. The catalogue specifies that the Δt parameter stands for the difference between the mean water temperature of the panels and the operative temperature of the room, which, in its simplified form, stands for the mean of the mean radiant temperature and the air temperature. In the present case, the adopted value for the operative temperature was provided by calculation from the measured data. The value of the operative temperature corresponds to the limit value obtained in a steady state regime. Mathematically this value stands to be the asymptotic one on the exponential growth of the operative temperature. This is the maximum operative temperature reached on the system and it can be considered as the project value on the moment of the calculus

for the selection of the radiant panel equipment like it is supposed to be done on the project procedure described on the Zehnder ZIP Catalog [19]. The graphic below (Figure 4.1) describes the reaching of the project temperature on the exponential growth.

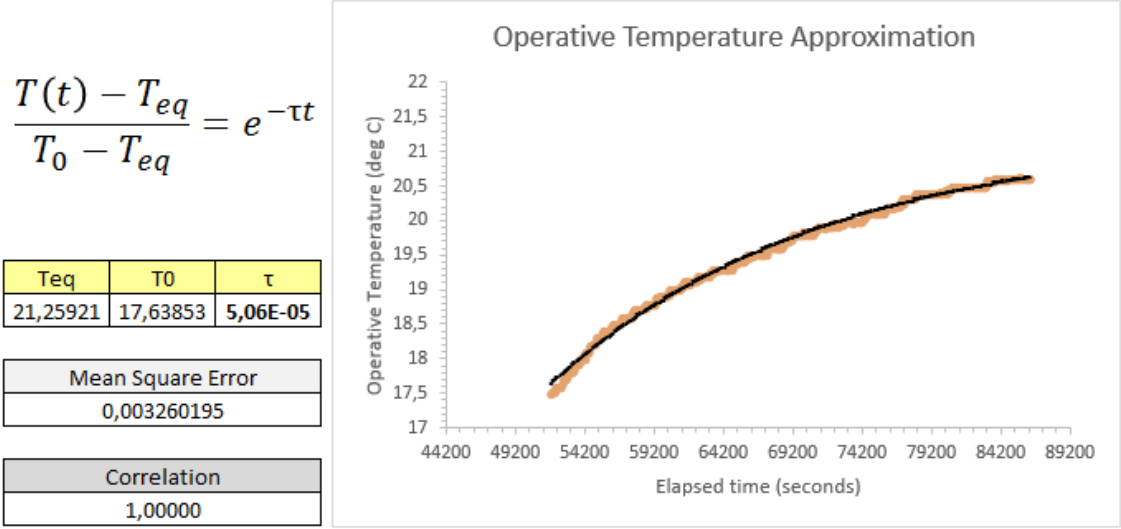


Figure 4.1. Operative temperature behaviour approximation.

It was realized an approximation procedure to make sure that the obtained value for the maximum operative temperature actually corresponds to the asymptotic one. There was executed the minimum square method to approximate the set of data to an exponential function, and as it is possible to see, the limit of that function is indeed the maximum operative temperature value obtained by measurement, about 22°C.

To obtain the ΔT_{power} , besides knowing the project operative temperature which stands for the temperature it is wanted the indoor climate to converge to, it is necessary to consider the water temperature, which, once again, is very similar to the radiant panel temperature in a steady state regime. Basically this temperature is the mean value of the inlet and the outlet temperatures, but once the inlet and the outlet water temperatures are periodic functions, it was necessary to proceed to the average value of each one like exposed on the Figure 4.2.

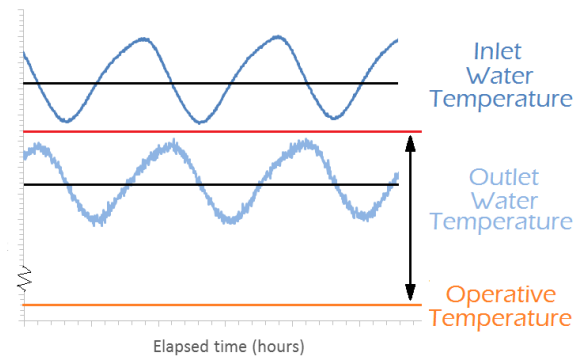


Figure 4.2. Obtainment of the temperature difference.

The temperature difference then obtained was about 54°C , after setting the water temperature to close than 75°C . After obtaining the ΔT_{power} value, it was searched on the project chart presented below (Figure 4.3) [19].

Potencia térmica con aislamiento				
	Placa ZIP Individual		ZIP2	
K	2,0871	0,2456	4,1742	0,4912
n	1,1489	1,3524	1,1489	1,3524
Δt (K)	W/m	W/par de colectores	W/m	W/par de colectores
80	321	92,0	641	184
56	213	56,8	426	114
55	208	55,4	417	111
54	204	54,1	408	108
52	195	51,4	391	103
50	187	48,7	374	97,5
48	178	46,1	357	92,3

Figure 4.3. Heating power calculation table for the radiant ceiling panels.

Comprehended between two values, it was necessary to make an interpolation in order to know the correspondent specific heating power value for the ZIP2 panels.

$$\Delta(\Delta T_{power}) = 2 \rightarrow \Delta(W/m) = 17$$

$$\Delta(\Delta T_{power}) = 53,57817 - 52 = 1,578167 \rightarrow \Delta(W/m) = x \approx 13 \text{ W/m}$$

Then:

$$\text{Specific Power} = 391 + 13,414 \approx 400 \text{ W/m}$$

So, as it can be seen, the specific power is about 400 W/m , which multiplied by the total length of the panels (16 meters) and, of course, considering that each of the 2 pairs of collectors transfers an amount of approximately 40W of heat, the total heating power of the radiant panels is about $6,6 \text{ kW}$.

$$Q = (16 \times 400) + (4 \times 40) \approx 6,6\text{kW}.$$

Where:

Q – heating power , in watt (W)

4.2. Estimating the Laboratory Thermal Parameters

Returning to the definition of this segment of the work, the objective is to identify the system looking at its variables and describe their behaviour mathematically. At this section the thermal model of the present system is going to be defined by the air temperature. By other words, to mathematically describe the system of the room plus the radiant panel circuit, is necessary to simplify it and make its definition for each different variable. In this case the simplified and equivalent model is represented in the picture bellow (Figure 4.4).

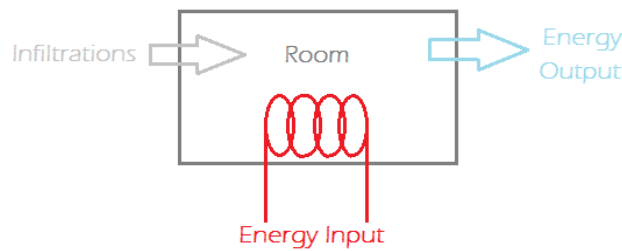


Figure 4.4. Equivalent model of the system.

As it's possible to see, in what concerns to the air of the room, in an HVAC application, more than the input of energy, a system is characterized by its response, but also, by its internal generations/gains and its infiltrations. Therefore, developing a model of the air mass affected by the radiant panels starts by a thermal energy balance defined by the following equations [20].

$$\frac{\partial Q}{\partial t} = m_a c_v \frac{\partial T_a}{\partial t} \quad (4.1)$$

$$m_a c_v \frac{\partial T_a}{\partial t} = Q_{panels} + Q_{infiltrations} + Q_{boundaries} \quad (4.2)$$

With:

$$Q_{panels} = k_q (\dot{m} c_{p,water} \Delta T_{water}) \quad (4.3)$$

$$Q_{infiltrations} = \rho V \lambda c_{p,air} (T_{ext} - T_a) \quad (4.4)$$

$$Q_{boundaries} = UA(T_{ext} - T_a) \quad (4.5)$$

Which results in:

$$\rho V c_v \frac{\partial T_a}{\partial t} = UA(T_{ext} - T_a) + \rho V \lambda c_{p,air}(T_{ext} - T_a) + k_q(\dot{m} c_{p,water} \Delta T_{water}) \quad (4.6)$$

Where:

A – room surface area, in square meters (m^2)

$c_{p,air}$ – specific heat at constant pressure of the air, in kelvin ($J/(kg \cdot K)$)

$c_{p,water}$ – specific heat at constant pressure of the water, in kelvin ($J/(kg \cdot K)$)

c_v – specific heat at constant volume of the air, in kelvin ($J/(kg \cdot K)$)

k_q – usage factor, dimensionless

\dot{m} – air mass flow, in kilograms per second (kg/s)

m_a – air mass, in kilograms (kg)

T_a – air temperature, in kelvin (K)

T_{ext} – external temperature, in kelvin (K)

U – global heat transfer coefficient, in watt per square meter kelvin ($W/(m^2 \cdot K)$)

V – room volume, in cubic meters (m^3)

ΔT_{water} – water temperature difference between inlet and outlet, in kelvin (K)

λ – infiltration rate, in seconds powered minus one (s^{-1})

ρ – air density, in kilograms per cubic meter (kg/m^3)

Observing the equation, there are 3 important parcels to consider in the present HVAC system, the balance related to heat exchange by the radiant panels (Q_{panels}), the infiltrations ($Q_{infiltrations}$) and the heat exchanges with the exterior ($Q_{boundaries}$). The usage factor corresponds to the portion of the heat energy which is converted in air temperature alteration (in this case).

Another commonly used portion in the energy balance is the internal gains part. The internal gains are important to consider once these gains come from the equipment that generate heat associated to their operation, like computers and screens. The internal gains, besides considering the heat transfer under the shape of conduction and convection, also consider heat transfer by radiation, as it happens with lighting. Additional work, as fan movement, is energy input and, for that reason, internal gains. Considering that the experiment room is a laboratory, this could be a very important factor to consider.

However in the present work, during the data acquisition, the screen and the computer only emitted an irrelevant amount of heat and the lights were maintained off. Also, there was no additional work in the system, therefore the internal gains part not considered in the thermal balance equation.

Apart of this parcel, the infiltrations are also important to consider on the great majority of HVAC systems. Basically, the infiltrations are leaks of air through windows and doors which varies the internal energy of the control volume. As well, as it influences the air mass. In fact, with no windows or doors opened, the only way of air renovation is by infiltration, that's why this portion of the energy comes as function of the infiltration rate (λ).

To adjust the equation of energetic balance to the set of data points of the air temperature, is necessary to solve the equation in order to the air temperature.

$$T_k = T_{k-1} + \frac{\Delta t}{\rho V c_v} \left[(UA + \rho V \lambda c_{p,air}) \cdot (T_{ext} - T_a) + k_q (\dot{m} c_{p,water} \Delta T_{water}) \right] \quad (4.7)$$

T_k – (k) value of air temperature, in kelvin (K)

T_{k-1} – (k – 1) value of air temperature, in kelvin (K)

The adjustment of the equation (4.16) to the set of air temperature points is made by the minimum square method, recurring to the Solver tool in order to minimize the difference by modifying the global heat transfer coefficient, the infiltration rate and the usage factor. The following graphic (Figure 4.5) is then representing the adjustment of the energetic balance to the set of points that best describe the normal operation of the radiant panels.

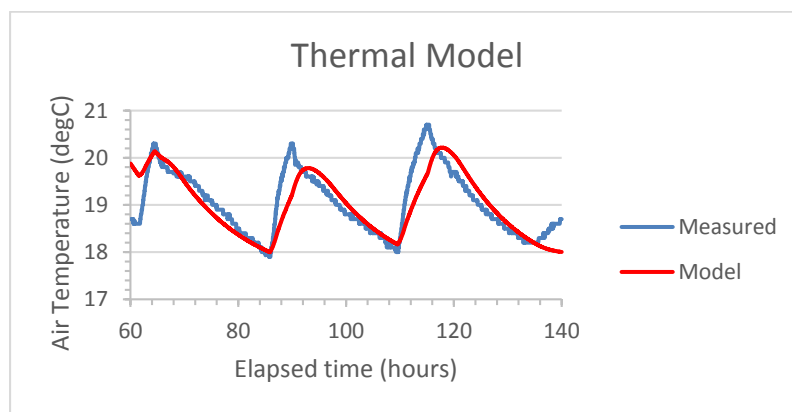


Figure 4.5. Thermal model approximation.

As it is seen, there is some delay in response between the measured values and the mathematical model, which affects the maximum values obtained by the equation. Obviously, on reality there is shuffle component that hardly can be modelled.

The obtained equation is:

$$617405,31 \frac{\partial T_a}{\partial t} = 2,30465(T_{ext} - T_a) + 53734,12(T_{ext} - T_a) + 70740,12\Delta T_{water}$$

Being:

$$U.A \approx 2,3 \text{ W/K}$$

$$k_q \approx 0,316$$

$$\lambda \approx 0,06 \text{ h}^{-1}$$

The global heat transfer coefficient (U) stands for the ability of surface barriers to transfer heat, so that it corresponds to the inverse of the resistance of those surfaces, whether in heat transfer by convection, whether by conduction. In this case, the value is quite low as expected once this coefficient corresponds to a transfer surface that, compared with the remaining surfaces, consists in a smaller area. The surfaces, through the energy contacts the exterior consist in walls, concrete beams and in wide windows. The determined usage factor (k_q) reveals that approximately 32% of the radiant panel energy is directly utilized to heat up the air, which corroborates the fact of about 60 to 70 percent of the energy being transferred by radiation as seen on the introduction on the Section 1.1.3. The obtained infiltration rate (λ) basically shows that, in one hour the system doesn't reach a renovation of a tenth of the air volume, which makes sense, since it is related only to the infiltrations.

Therefore, in result, the energetic balance depends on the actual air temperature, the external temperature and the water temperature difference. Such mathematical model is significantly important in an application of a monitoring and control system, since is that equation that best describes the behaviour of the system allowing the monitoring and control module to act at the right moment by prevision. Remembering, one of the objectives of this work is to make it possible to attach a controlling device on the radiant panel circuit in order to connect and disconnect the flow and control the bypass valve, obviously maintaining the thermic comfort on the laboratory. Such tasks can be realized by a proportional-integral-derivative (PID) control method which precisely requires an

equation of this type. Being differential, the temperature obtained values follow a behaviour already affected by increasing or decreasing tendencies, since it depends, as the names says, of the first derivative. This is one of the reasons why a certain delay is shown in the model approach.

4.3. System Performance in terms of the Occupancy

The main reason why monitoring and controlling is so important in HVAC systems is to turn them more energy efficient but always focusing on stablishing thermal comfort, therefore, the key is in the occupation profile in how people really feel. This segment of the work is where it is acquired a notion on the thermal comfort and, in order to do that, it is necessary to recur to more subjective methods of system identification and evaluation, such as the predicted mean vote (PMV) and the predicted percentage of dissatisfied people (PPD) described at the Appendix A of this work. The PMV index was calculated in an Octave program (presented at the annex C) recurring to the method of Fanger, described in the Appendix A, and then exported to an Excel calculus sheet. Remember that the Fanger's method consists in an iterative method, so that is impossible to proceed on the calculus of thousands of data lines in a calculus sheet. In order to calculate the PMV index, beyond the measured data it was required the establishment of two parameters: the metabolism (m) and the basic clo value (I_{cl}). This values were picked from a chart presented on the ISO7730 norm [17] (see Appendix A), which are following represented.

$$\therefore m = 1,2 \text{ met}$$

$$I_{cl} = 1 \text{ clo (work clothing)}$$

As result, the graphic representation of the PMV values is following represented in the Figure 4.6.

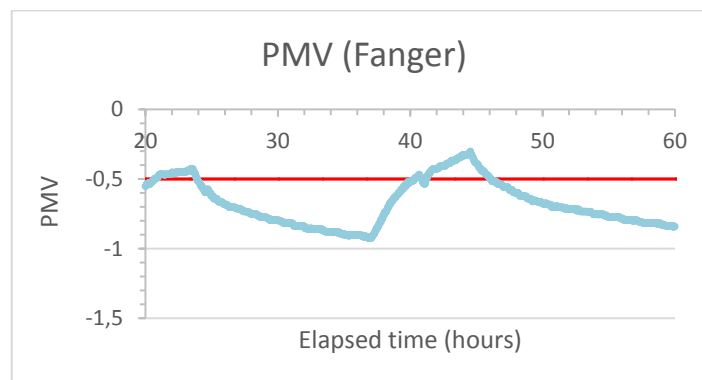


Figure 4.6. PMV response (calculated by Fanger's method).

The values represented in the graphic correspond to the ones calculated recurring to the medium radiant temperature obtained by the standard globe temperature. However, as already referred, this response is very similar to a response provided by the little globes' temperature. Comparing this data with previous graphics of operative temperature and medium radiant temperature, the behaviour is directly proportional and the shape of the representation is also a sequence of exponential increases and decreases.

As it is possible to observe, without the radiant panel circuit on, the PMV becomes near -1 in the end of the winter, which means, as expected, people tend to feel cold, but surprisingly, not so significantly. Also expected, after heating the indoor space, the PMV acquires values closed to 0, which is what is intended for thermal comfort. In fact, the ideal comfort zone stands between $-0,5$ and $0,5$, whose inferior limit is represented on the graphic zone. As shown, the indoor space is able to get a considerable value of hours on the ideal comfort zone and those hours correspond to the occupation period of the laboratory. Still, it can be concluded that, against the expectation on the preliminary analysis, the radiant panels are not supplying too much heat, instead, they could actually provide more heat to the room in order to have more hours of operation in the ideal thermal comfort zone.

As simple as the result might be, not so simple is the PMV calculus by the Fanger method, so a new work line of thought was created in order to simplify the calculation process. It turns out that it does exist a simplified method for PMV calculation. Proposed by Max Sherman [18], the simplified method recurs to a set of coefficients which are the result of three main simplifications.

The applied simplifications were the linearization of radiation, the consideration of a standardized dew-point value and the simplification of the convection coefficient. This simplifications basically surpass the iterative calculus by turning the equation into a linear expression, incorporating the humidity effect without relation to air temperature itself and making the convection coefficient independent of the clothes' temperature. This last one is a characteristic that, as referred in the article, allows the implementation of PMV calculus in control algorithms to large HVAC systems, in thermal comfort based controllers, which is precisely the intended for the present case.

The equation for the calculation of PMV with the Sherman method is the following one.

$$Y = Y_o + Y_r \frac{MRT}{T_s} + Y_c \frac{T_d}{T_s} + Y_e \frac{T_d^2}{T_s^2} \quad (4.8)$$

Where:

MRT – mean radiant temperature, in degrees Celsius ($^{\circ}C$)

T_d – dew – point temperature, in degrees Celsius ($^{\circ}C$)

T_s – skin temperature, in degrees Celsius ($^{\circ}C$)

Y – predicted mean vote (Sherman's method), dimensionless

Y_c – convective comfort coefficient, dimensionless

Y_e – evaporative comfort coefficient, dimensionless

Y_o – basic comfort coefficient, dimensionless

Y_r – radiative comfort coefficient, dimensionless

Therefore, the only measured data required to the PMV calculation by the present method are the mean radiant temperature, the air temperature and the dew-point. In reality, in the realized experiment, the humidity level was well measured due to the noise and instability of the humidity sensor, therefore, the adopted value of dew-point consists in an approximated constant value. This constant value was adopted having in mind the exterior conditions for the period of the experiment, analysed on the website of meteorological station of the department, near the laboratory [21]. In the end, it was considered a dew-point of $5^{\circ}C$, which consists in a proper value for the last weeks of winter and on indoor climate. It's known that this should be a measured parameter but an approximated value consists in a good approach since the humidity doesn't significantly affect the PMV value in [22].

Finally, the skin temperature, as defined in this method, doesn't depend on the exterior conditions, but on the metabolism, which corresponds to a constant value picked up from the same tabulated standard values that are utilized by the Fanger's method.

Finally, the results of the PMV calculation with the Sherman method are following represented, in the Figure 4.7.

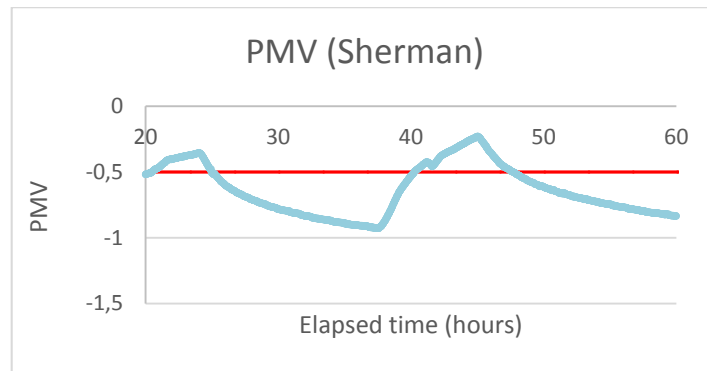


Figure 4.7. PMV response (calculated by Sherman's method).

Corresponding to the expectations, the result was an almost perfect match when comparing the PMV values obtained with the Sherman method with the ones obtained by the Fanger's calculation. As it is possible to see in both graphics, on the Fanger's case, the PMV values are, the majority of the time, below the inferior limit of the ideal thermal comfort zone, like it is observed in the Sherman case. The error associated to this approximation is about 3 hundredths, which is nothing significant comparing to the size of the PMV scale. For that reason it was possible to validate, in the present work the simplification of the PMV calculus in order to develop the system identification of the radiant panel system. This consists in a great simplification that might allow a future monitoring and control system to be more practical, but equally efficient.

The other important thermal comfort index, the PPD, was also calculated in the Octave program, recurring, therefore, to the PMV values obtained with the Fanger's method. Recurring to Equation (6.22) presented in the Appendix A, the results of the PPD calculation are presented in the following graphic (Figure 4.8).

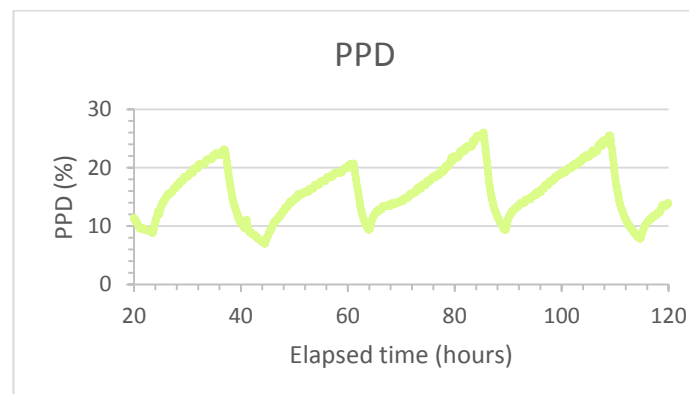


Figure 4.8. PPD response.

As it was expected, the same exponential behaviour is shown for PPD, however, comparing this results with the graphic from the Figure 4.6, this evolution is in phase opposition to the PMV. As the PMV grows, the PPD decreases and vice-versa. Well this behaviour is logical, knowing that in an initial stage, people feel cold, when the PMV level gets higher, by other words, when the environment heats, the predicted percentage of dissatisfied people decreases once the occupants tend to feel more comfortable and, obviously, the more colder it is, the more dissatisfied people are. But note that this relation happens only when exists the need for heating. On the opposite situation, for example in summer, the higher the PMV gets, the higher the PPD becomes, by the same logic.

Another conclusion is that during the working period of the radiant panels the predicted percentage of dissatisfied people is close to 10% while, during non-operation time the PPD is about 24% approximately, which means that the operation of the radiant panels has a significant meaning for 14% of the occupants.

5. CONCLUSIONS

As observed, in the present work, a radiant ceiling panel system have been defined by a first order response based thermal model, being meanwhile the object of an approach to the thermal comfort evaluation in the experimental context. After the analysis of the characteristic variables and the power output calculation of the circuit, the following conclusions were acquired:

1. In a controlling absence, the system might get an accumulation of energy that for a long time of continuous operation which has to be considered on future control approaches.
2. The air temperature vertical distribution is, indeed, very uniform as a result of the relative low influence on the radiant heating on the air mass.
3. The obtained thermal model revealed that the present equipment releases about 31,58% of the water energy directly to the surrounding air.
4. The obtained thermal model is able to follow the behaviour of the air temperature with sufficient accuracy.
5. More accessible instrumentation can be applied in order to acquire the operative and mean radiant temperatures.
6. The PMV index, as a control variable, can be calculated with a simpler method without significantly compromising the precision of the results.
7. During the operation of the radiant panel system, the predicted percentage of dissatisfied people is close to 10%, therefore, near to the limit of the reasonable performance value.

In this study, it was possible to obtain basic necessary parameters that can be further utilized on the monitoring and control of RHC systems independently of its background properties, as well as practical sensing perspective in order to turn the operation of this devices a much efficient process.

It is believed that this work consist in an information source which might be useful and can be followed in future work:

- Thermal model acquisition for the remaining system variables (mean radiant temperature, operative temperature and predicted mean vote);
- Development of a control algorithm in order to control the basic operation of the radiant ceiling panel circuit, as well as its bypass, based on thermal comfort establishment;
- Simulation and testing of the control algorithm;
- Implementation of a monitoring and control system on the present circuit;
- Optimization of the monitoring and control system of the laboratory panel circuit based on people's reaction and feedback.

BIBLIOGRAPHY

- [1] Zehnder, “Guide on energy savings from ceiling-mounted heating and cooling systems”. Technical Catalogue.
- [2] B. R. Bean, M. Ashrae, B. W. Olesen, D. Ph, F. Ashrae, K. W. Kim, D. Arch, “History of Radiant Heating & Cooling Systems (Part 2),” no. January, 2010.
- [3] B. R. Bean, M. Ashrae, B. W. Olesen, D. Ph, F. Ashrae, K. W. Kim, D. Arch, “History of Radiant Heating & Cooling Systems (Part 1),” no. January, 2010.
- [4] <http://www.google.com/patents/US4080703>; Accessed on 2 of July of 2015
- [5] <http://www.google.com/patents/EP0961084A1?cl=en>; Accessed on 2 of July of 2015
- [6] <http://www.google.com/patents/US20090314463>; Accessed on 2 of July of 2015
- [7] M. N. Alban, “LITERATURE STUDY ON RADIANT HEATING IN A THERMALLY-COMFORTABLE INDOOR ENVIRONMENT”, September 2010. (http://www.ducoterra.com/wp-content/uploads/2014/05/summ_report_study_kul_rad_heat.pdf; Accessed on 2 of July of 2015)
- [8] E. F. Bell, “Infant incubators and radiant warmers.,” *Early Hum. Dev.*, vol. 8, no. 3–4, pp. 351–375, 1983.
- [9] S. Cho, M. H. Shin, Y. K. Kim, J.-E. Seo, Y. M. Lee, C.-H. Park, and J. H. Chung, “Effects of infrared radiation and heat on human skin aging in vivo.,” *J. Investig. Dermatol. Symp. Proc.*, vol. 14, no. 1, pp. 15–19, 2009.
- [10] T. Imanari, T. Omori, and K. Bogaki, “Thermal comfort and energy consumption of the radiant ceiling panel system. Comparison with the conventional all-air system,” *Energy Build.*, vol. 30, no. 2, pp. 167–175, 1999.
- [11] S. Seyam, A. Huzayyin, H. El-Batsh, and S. Nada, “Experimental and numerical investigation of the radiant panel heating system using scale room model,” *Energy Build.*, vol. 82, pp. 130–141, 2014.
- [12] K. Rhee and K. Woo, “A 50 year review of basic and applied research in radiant heating and cooling systems for the built environment,” *Build. Environ.*, vol. 91, pp. 166–190, 2015.

- [13] Mikron Instrument Company, "Total emissivity of various surfaces for infrared thermometry" (http://www-eng.lbl.gov/~dw/projects/DW4229_LHC_detector_analysis/calculations/emissivity2.pdf; Accessed on 2 of July of 2015)
- [14] Bruel & Kjaer, "Instruction Manual - Indoor Climate Analyzer type 1213"
- [15] ISO 7726. 1998, "Ergonomics of the thermal environment - Instruments for measuring physical quantities", Geneva.
- [16] <http://www.infrared-thermography.com/material-1.htm>; Accessed on 2 of July of 2015
- [17] ISO 7730. 2005, "Ergonomics of the thermal environment - Analytical determination and interpretation of thermal comfort using calculation of the PMV and PPD indices and local thermal comfort criteria", Geneva.
- [18] M. Sherman, "A simplified model of thermal comfort," *Energy Build.*, vol. 8, no. 1, pp. 37–50, 1985.
- [19] Zehnder, "Zehnder ZIP - Sistemas de calefacción y refrigeración por techo radiante (Catálogo técnico)"
- [20] L. Torres and M. L. Martin, "Adaptive Control of Thermal Comfort Using Neural Networks." (http://www.inaut.unsj.edu.ar/Files/To1810_08.pdf; Accessed on 2 of July of 2015)
- [21] <http://www.wunderground.com/personal-weather-station/dashboard?ID=ICOIMBRA14#history/s20150217/e20150319/mmonth>; Accessed on 2 of July of 2015
- [22] R. Moutela, João Dias Carrilho and Manuel Gameiro da Silva, "SENSITIVITY OF THE PMV INDEX TO THE THERMAL COMFORT," pp. 14–15, 2015.
- [23] A. C. Pereira, "Simulação dinâmica do comportamento termo-higrométrico de superfícies radiantes hidráulicas para aquecimento e arrefecimento ambiental," pp. 1–58, 2004.
- [24] ASHRAE, ASHRAE Handbook - Fundamentals. Atlanta, GA: American Society of Heating, Refrigerating and Air Conditioning Engineers; 2001.
- [25] ASHRAE, ASHRAE Handbook - Heating, Ventilating and Air Conditioning Applications. Atlanta, GA: American Society of Heating, Refrigerating and Air Conditioning Engineers; 1999.
- [26] Bruel & Kjaer, "Application Notes - Evaluation of Moderate Thermal Environments"

APPENDIX

A – Descriptors of Thermal Comfort

Plane Radiant Temperature

For the calculus, is important to start by the following definition of the net radiation [15].

$$P = \sigma(T_{prA}^4 - T_{prB}^4) \quad (6.1)$$

Where:

P – net radiation, in watts per square meter (W/m^2)

σ – Stefan

– Boltzmann constant, in watts per square meter kelvin to the fourth power

$$[\sigma = 5,67 \times 10^{-8} W/(m^2 \cdot K^4)]$$

T_{prA} – plane radiant temperature on side A, in kelvin (K)

T_{prB} – plane radiant temperature on side B, in kelvin (K)

By definition,

$$\Delta t_{pr} = T_{prA} - T_{prB} \quad (6.2)$$

Where:

Δt_{pr} – radiant temperature asymmetry, in kelvin (K)

This quantity isn't determined directly by the transducer, whereby it has to be calculated in the analyser module.

Continuing, the Equation (6.1) can be written as:

$$P = 4\sigma T_n^3 (T_{prA} - T_{prB}) \quad (6.3)$$

In this equation, the $(4\sigma T_n^3)$ factor is defined as the linear radiant heat transfer coefficient, where $T_n = 0,5(T_{prA} + T_{prB})$ or equal to the transducer's temperature, to be more precise.

Where:

T_n – net radiometer's temperature, in kelvin (K)

From the Equation (6.3), the radiant temperature asymmetry becomes

$$\Delta t_{pr} = \frac{P}{4\sigma T_n^3} \quad (6.4)$$

Translated in words, the radiant temperature asymmetry is, obviously, a function of irradiation, but dependent of the linear radiant heat transfer coefficient which, by its turn, is influenced by the level of temperature represented as T_n . At the temperature level of the present system, which corresponds to 20°C, the coefficient is equal to 5,7 W/(m². K).

Then, to obtain the formula for the calculus of the plane radiant temperature, it is necessary to consider each side independently, so that, the following equation represents the value of the irradiation on a single side of the net radiometer, by other words, when radiation heat transfer is only measured in one side.

$$P = \sigma T_{pr}^4 - \sigma \varepsilon_s T_n^4 \quad (6.5)$$

Where:

ε_s – emissivity of the sensor

Once again, for a black painted element, the emissivity is considered to be approximately 0,95.

Solving the previous equation in order to T_{pr} , the plane radiant temperature becomes:

$$T_{pr} = \sqrt[4]{0,95T_n^4 + \frac{P}{\sigma}} \quad (6.6)$$

In the end, this corresponds uniquely to one side of the transducer. To obtain the radiant temperature asymmetry, it is necessary to measure on both sides to obtain the difference.

Mean Radiant Temperature

The Mean Radiant Temperature is defined as “the uniform temperature of the surrounding surfaces of an imaginary enclosure where the radiant heat transfer between the space and the occupant is equal to the sum of the non-uniform radiant heat transfers from the surrounding surfaces of the real space”[23]. By other words, it’s the mean value of the temperature that is actually felt exclusively from radiation. As the PMV index was indicated to be, the MRT is a control variable to serve as reference for the radiant panel control project and its behaviour is very relevant to the system identification. As explained

on the introduction, the radiant heat transfer corresponds to a very significant part of the mechanisms of heat transmission, once all the present bodies in a room, and inclusively the room itself, emit and absorb radiant energy that promotes climate temperature changes. Whereby, the Mean Radiant Temperature corresponds to the sum of the temperatures of each surrounding element (walls, floor, windows, furniture...) multiplied by the apparent surface area of those elements and divided the sum of these same areas. Well, as it's easy to conclude, in complex systems full of several elements with different shapes and emissivity values, it would be an extremely hard job to evaluate the MRT by shape factor based calculus. Well, in reality, the Mean Radiant Temperature is measured with a black globe sensor.

The globe temperature (t_g) corresponds to the temperature at the centre of the hollow sphere which is equal to the mean temperature of the surface. This external surface is generally coated by an electro-chemical process to acquire that finish of matt black paint, must be as thin as possible and has an emission coefficient of approximately 0,95. These globes are capable of measuring up to 120 °C and their accuracy is around 0,5 °C to 1 °C depending on the temperature range.

Basically these globes receive the radiation from de surroundings but also consider heat exchanges by convection between the air and itself, which causes a heat balance to consider. Note that this globes are specified to be thin enough to consider that the temperature of the inner surface of the globe and the temperature of the surrounding air are practically equal to the average temperature of the external surface of the globe. The thermal exchanges' balance between the globe and the environment are given in the following equation:

$$q_r + q_c = 0 \quad (6.7)$$

Where:

q_c – convective heat exchange, in watts per square meter (W/m^2)

q_r – radiant heat exchange, in watts per square meter (W/m^2)

Summing up, this equality is possible due to the inexistence of convection in the interior of the globe, so that every radiant exchanges are equivalent to every convective exchanges outside the globe, once it is considered the frontier temperatures to be equal.

The heat transfer by radiation between the globe and the walls, as well as every objects, of the enclosure can be defined by the mean radiant temperature and the globe temperature, as it's possible to see on the following equation.

$$q_r = \varepsilon_g \sigma (MRT^4 - T_g^4) \quad (6.8)$$

Where:

T_g – Temperature of the black globe, in kelvin (K)

ε_g – emissivity of the globe's surface, dimensionless

The heat transfer by convection between the globe and the air of the room is defined by the next equation.

$$q_c = h_{cg} (T_a - T_g) \quad (6.9)$$

Where:

h_{cg}

– convection coefficient at the level of the globe, in watts per square meters kelvin (W/(m². K))

In natural convection, this coefficient corresponds to:

$$h_{cg} = 1,4 \left(\frac{\Delta T}{D} \right)^{1/4} \quad (6.10)$$

Knowing that:

$$\Delta T = T_g - T_a$$

Where:

ΔT – Difference between the globe and the air temperatures, in kelvin (K)

And in forced convection:

$$h_{cg} = 6,3 \frac{v_a^{0,6}}{D^{0,4}} \quad (6.11)$$

Where:

D – diameter of the globe, in meters (m)

v_a – air velocity at the level of the globe, in meters per second (m/s)

Therefore, in our case, it stays:

$$h_{cg} = 1,4 \left(\frac{\Delta T}{0,15} \right)^{1/4}$$

And:

$$h_{cg} = 6,3 \frac{v_a^{0,6}}{0,15^{0,4}}$$

The procedure to adopt on the calculus of this convection coefficient is to calculate it utilizing both formulas and then choosing the bigger value. In the present work, it is not obvious what model (natural or forced convection) to adopt, and this is the point when it reveals important to measure the air velocity.

Now, substituting the Equations (6.8 and 6.9) on the Equation (6.7), we obtain the following result for the thermal balance of the black globe:

$$\varepsilon_g \sigma (MRT^4 - T_g^4) + h_{cg} (T_a - T_g) = 0 \quad (6.12)$$

Solving this in order to MRT, we obtain:

$$MRT = \sqrt[4]{T_g^4 + \frac{h_{cg}}{\varepsilon_g \sigma} (T_g - T_a)} \quad (6.13)$$

The next conversion depends on the use of the convection coefficient, if it corresponds to natural or to forced convection.

For the natural convection, one obtains:

$$MRT = \left[(T_g + 273)^4 + \frac{0,25 \times 10^8}{\varepsilon_g} \left(\frac{|T_g - T_a|}{D} \right)^{1/4} \times (T_g - T_a) \right]^{1/4} - 273 \quad (6.14)$$

Which, in this case, for the standard black globe ($D = 0,15m$ e $\varepsilon_g = 0,95$), becomes:

$$MRT = \left[(T_g + 273)^4 + 0,4 \times 10^8 |T_g - T_a|^{1/4} \times (T_g - T_a) \right]^{1/4} - 273$$

Next, for the forced convection, it becomes that:

$$MRT = \left[(T_g + 273)^4 + \frac{1,1 \times 10^8 \times v_a^{0,6}}{\varepsilon_g \times D^{0,4}} \times (T_g - T_a) \right]^{1/4} - 273 \quad (6.15)$$

Once, again, for the standard globe, the Equation (6.15) becomes:

$$MRT = \left[(T_g + 273)^4 + 2,5 \times 10^8 \times v_a^{0,6} (T_g - T_a) \right]^{1/4} - 273$$

Like the standard globe, it is possible to calculate the MRT through the Equations (6.14 and 6.15), for other size globes, whether the convection is natural or forced. For the small Thermokon globes with 40 mm diameter and glossy finish, the following simplified models of those equations here presented were obtain considering ($D = 0,04m$ e $\varepsilon_g = 0,92$).

For the natural convection:

$$MRT = \left[(T_g + 273)^4 + 0,607627 \times 10^8 |T_g - T_a|^{1/4} \right. \\ \left. \times (T_g - T_a) \right]^{1/4} - 273 \quad (6.16)$$

For the forced convection:

$$MRT = \left[(T_g + 273)^4 + 4,332922 \times 10^8 v_a^{0,6} \right. \\ \left. \times (T_g - T_a) \right]^{1/4} - 273 \quad (6.17)$$

Operative Temperature

The Operative Temperature might be understood as the temperature of an hypothetic enclosure where the air temperature is equal to the medium radiant temperature and the heat exchanges by radiation and convection, between the environment and the person, is the same as the real environment. In practice, the Operative Temperature is the combined result of the measurement of the air and medium radiant temperatures [15] [24] and the exact equation to determine it is:

$$T_{op} = \frac{h_c \cdot T_a + h_r \cdot MRT}{h_c + h_r} \quad (6.18)$$

Where:

h_c – convective heat transfer coefficient, in watts per square meter kelvin [W / (m². K)]

h_r – radative heat transfer coefficient, in watts per square meter kelvin [W / (m². K)]

T_{op} – operative temperture, in kelvin (K)

The radiative heat transfer coefficient is defined by the following equation [25]:

$$h_r = 4\sigma_{\text{eff}} \left[\frac{(MRT - T_a)}{2} + 273 \right]^3 \quad (6.19)$$

Where:

f_{eff} – ratio of radiating surface of the human body to its total DuBois surface area
 $= 0,71$

By its turn, the convective heat transfer coefficient is defined by the equation below [25].

For forced convection:

$$h_c = 8,5v_a^{0,5} \quad (6.20)$$

For natural convection:

$$h_c = 12,1\sqrt{v_a} \quad (6.21)$$

Dew-Point Temperature

For any context of thermal comfort monitoring and control, the dew-point is an important variable to measure once it directly affects the human thermoregulation. In warm environments, the human body uses sweat as a chill solution through its evaporation rate. Of course, this rate depends on the present humidity in the air and on how much water-vapour the atmosphere still can carry. By other words, if the air is saturated, the sweat doesn't evaporate and it accumulates on the skin surface, causing discomfort. And still, the human body produces sweat at the same rate as if it was evaporating. Basically this is the reason why people might sweat in humid days even if it's not so warm. It all depends on the dew-point. Bigger concentrations of humidity in the air mean less difficulty to occur condensation at the same pressure and, by its turn, mean higher temperatures of that phenomena. However, too dried air environments can cause skin irritation and respiratory tract dryness, so that the norms establish an ideal range for the dew-point to ensure thermal comfort (between $-4,5^{\circ}\text{C}$ and $15,5^{\circ}\text{C}$).

Predicted Mean Vote and Predicted Percentage of Dissatisfied

The PMV (Predicted Mean Vote), as the name says, stands for the mean thermal vote of a large group of people on the same environment and consists on one hypothetical control variable to serve as reference to the controlling algorithm for the radiant panels. The classifying grid or scale is represented in the Figure 0.1.

+ 3	Hot
+ 2	Warm
+ 1	Slightly warm
0	Neutral
- 1	Slightly cool
-2	Cool
- 3	Cold

Figure 0.1. PMV scale.

As it is possible to see through the image, people who feel colder tend to vote on the lowest levels of the scale and, of course, people who feel warmer tend to vote on the highest levels of the scale. Therefore, it turns that the zero grade is the most comfortable level, so that it is the reference to adjust the indoor climate. More specifically, the ideal thermal comfort level is in the range of PMV from -0,5 to +0,5, as these are the limits recommended by the norm ISO 7730 (as consulted on the manual [26]).

Although this method of thermal comfort characterization is very intuitive and closed to the common person, it is also, on the other hand, very subjective once it depends from people to people, whether psychologically or physically (through differences on gender, activity/metabolism, clothing and thermoregulation).

As this is a method that can be mathematically treated as a normal model of probability distribution due to the fact all the votes are scattered around a mean value, it is possible to predict the number of people likely to feel uncomfortable (colder or warmer), and those are the ones that we must focus the attention on, once those are the people who are going to complaint about the environment.

In order to formally foresee that situation, there is the PPD factor (Predicted Percentage of Dissatisfied) that stands for, the probable percentage of people who are going to be dissatisfied with the climate and it's obtained by the mathematical method previously referred. The predicted percentage of dissatisfied people can calculated, depending on the PMV value through the following equation.

$$PPD = 100 - 95 \cdot e^{(-0,03353 \cdot PMV^4 - 0,2179 \cdot PMV^2)} \quad (6.22)$$

PMV – Predicted Mean Vote, dimensionless

PPD – Predicted Percentage of Dissatisfied, in percentage (%)

A value of PPD is considered reasonable if it is under 10%, as referred by the ISO 7730 norm [17].

To get to the PMV value, the sensor only measures, as said before, the air temperature, air velocity and the medium radiant temperature, but those values are constantly introduced in the following equations [17]:

$$\begin{aligned}
 PMV = & [0,303 \cdot \exp(-0,036 \cdot M) + 0,028] \cdot \{(M - \\
 & W) - 3,05 \times 10^{-3} \cdot [5733 - 6,99 \cdot (M - W) - p_a] - \\
 & 0,42 \cdot [(M - W) - 58,15] - 1,7 \times 10^{-5} \cdot M \cdot (5867 - p_a) - \\
 & 0,0014 \cdot M \cdot (34 - T_a) - 3,96 \times 10^{-8} \cdot f_{cl} \cdot [(t_{cl} + 273)^4 - \\
 & (MRT + 273)^4] - f_{cl} \cdot h_c \cdot (t_{cl} - T_a)\} \quad (6.23)
 \end{aligned}$$

$$\begin{aligned}
 t_{cl} = & 35,7 - 0,028 \cdot (M - W) - I_{cl} \cdot \{3,96 \times 10^{-8} \cdot f_{cl} \cdot [(t_{cl} + \\
 & 273)^4 - (MRT + 273)^4] - f_{cl} \cdot h_c \cdot (t_{cl} - T_a)\} \quad (6.24)
 \end{aligned}$$

Note that this equation corresponds to an iterative calculus of the clothing surface temperature, once this variable is represented by t_{cl} present in both members of the equation.

Where:

f_{cl} – clothing surface area factor

M – metabolic rate, in watts per square meter (W/m^2)

p_a – water vapour partial pressure, in pascal (Pa)

t_{cl} – clothing surface temperature, in degrees Celsius ($^{\circ}C$)

W – Effective mechanical power, in watts per square meter (W/m^2)

Note that:

$$1 \text{ metabolic unit} = 1 \text{ met} = 58,2 \text{ W/m}^2$$

$$1 \text{ clothing unit} = 1 \text{ clo} = 0,155 \text{ m}^2 \cdot \text{K/W}$$

It's easy to see that the equation for the PMV calculation depends on several subjective factors. Some values, such as the metabolic rate and the clothing insulation, are inclusively established by the measurer concerning to the conditions of the experimental context, through proper data tables following presented, Figure 0.2 and Figure 0.3.

Activity	Metabolic rate	
	W/m ²	met
Reclining	46	0,8
Seated, relaxed	58	1,0
Sedentary activity (office, dwelling, school, laboratory)	70	1,2
Standing, light activity (shopping, laboratory, light industry)	93	1,6
Standing, medium activity (shop assistant, domestic work, machine work)	116	2,0

Figure 0.2. Metabolic rates table.

Work clothing	I_{cl}		Daily wear clothing	I_{cl}	
	clo	m ² · K/W		clo	m ² · K/W
Underpants, boiler suit, socks, shoes	0,70	0,110	Panties, T-shirt, shorts, light socks, sandals	0,30	0,050
Underpants, shirt, boiler suit, socks, shoes	0,80	0,125	Underpants, shirt with short sleeves, light trousers, light socks, shoes	0,50	0,080
Underpants, shirt, trousers, smock, socks, shoes	0,90	0,140	Panties, petticoat, stockings, dress, shoes	0,70	0,105
Underwear with short sleeves and legs, shirt, trousers, jacket, socks, shoes	1,00	0,155	Underwear, shirt, trousers, socks, shoes	0,70	0,110
Underwear with long legs and sleeves, thermo-jacket, socks, shoes	1,20	0,185	Panties, shirt, trousers, jacket, socks, shoes	1,00	0,155
Underwear with short sleeves and					

Figure 0.3. Table of thermal insulation for typical combinations of garments.

Those are not pre-established on the thermal comfort transducer, but, instead, they depend on later indications from the user that sets the proper type of environment (concerning to occupancy) to measure. Of course if it is set the PMV value to zero and obtained the thermal comfort equation giving several combinations of all the factors considered on the calculus which correspond to thermal neutral sensation and to the optimal Operative Temperature. For example, it can recommend the users to use another type of clothing or moderate the activity, but this is not the usual procedure, because, in reality the indoor climate must be the one to adapt to the human occupancy. A situation where this might be important is, for example, during the project of infrastructures, where this thermal comfort equation might indicate us to utilize a different pavement or to coat the wall with a material more or less reflective or conductive to moderate the heat transfer rate.

B – Instrumentation Description

The first presented sensors are the ones related to the exterior and water temperatures (the models AGS54 and AKF10 from Thermokon, respectively), represented in the following picture (Figure 0.4).



Figure 0.4. Representation of the AGS54 and AKF10 sensors.

These two sensors work with the same principle, the variation of the electric resistance of the material (in this case, platinum) with the temperature. What happens is that, knowing these models have a positive temperature coefficient (PTC), as long as the temperature increases, the resistance of the material increases proportionally. Next, both sensors give us the signal in resistance variation, but what is measured in reality is a voltage, so that is necessary to read this value through a signal conditioner developed for RTDs, which consists of a Kelvin bridge with voltage reader and the excitation current terminals.

Concerning to the BK1213 module, there were utilized several transducers. Starting with the air temperature transducer, this is an RTD sensor with a PT100 resistance, therefore that means this platinum based has a 100 ohms resistance, which is the most common on RTDs. As it is possible to observe in the Figure 0.5, the sensible element of the transducer is surrounded by an open cylindrical shield which reflects the majority of the radiation, therefore reducing significantly the radiant heating effect on the sensible resistor, in order to obtain uniquely and exclusively the values of the dry bulb temperature, based in the process already described for RTD sensors. In fact, the unique difference

between this transducer and the ones described before is that, in this case, the sensible material is in contact with the air, instead of a surface or liquid.



Figure 0.5. Air temperature transducer.

Another parameter that involves the air itself is the air velocity. For the measurement of this displacement, it is necessary an air velocity transducer or anemometer. In the experimental assembly defined for this work, two types were used, they are a little bit different in shape and material.

Continuing with the BK1213 analyser, the anemometer which is attached to this module is the type MM 0038 and operates in the constant temperature mode. This principle establishes that the temperature to be constant is the one from the transducer sensible material. In this case, there are two coils in the instrument, one to be heated by input power and one without thermoregulation. Air displacement causes a higher heat transfer rate and, of course, heat loss on the sensible element. So that, the air velocity value is proportional to the necessary power input to maintain a constant temperature difference between both sensible elements, which is 15 °C according to what is specified on the analyser’s instruction manual [14]. Although this RTD sensor reveals to have an excellent sensitivity, the heat losses are, simultaneously, affected by the temperature and the direction of the flow, and are also a function of the surroundings radiative exchange. Basically those are sources of errors that can be eliminated with the proper design of the transducer. This device, presented in the Figure 0.6, is constituted by two sensitive ellipsoidal bodies which are disposed with an optimized eccentricity and length to highly reduce variation in directional sensitivity.

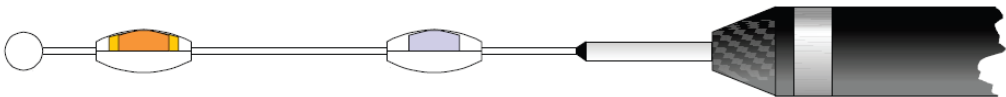


Figure 0.6. MM0038 anemometer.

Still, concerning the air velocity measurement, another sensor was used and consists, as well as the first one, in a heated anemometer, the Swema model 03, represented in the Figure 0.7. The sensor element consists in a PT100 resistance temperature device and the main difference in its shape is the protector shield composed by six thicker wires that form a protection cage, as it is possible to observe in the following picture. The main difference between both anemometers is the response time.



Figure 0.7. Swema's anemometer.

In the present work, two types of data, obtained with this hot wire anemometer, were logged: the air velocity and the temperature. Well, to determine the air temperature, the required principle is exactly the same. Note that, the more the air temperature is reduced (which can occur through air displacement), the more significant the power input in the wire to maintain its temperature. Once again, the air temperature is a function of the same power input necessary to determine the air velocity.

Relatively to the BK1213, the last sensor to describe is the thermal comfort transducer. This transducer is an elliptical body which is heated (see Figure 0.8), properly designed to simulate the relation between convection and radiation heat losses on human beings, so that the angle factors of the instrument and of humans are equivalent. For that to be done, it measures a quantity that is a function of heat exchange with the surrounding environment through convection and radiation, giving a measurement of Operative Temperature (defined in the appendix A).



Figure 0.8. Thermal comfort transducer.

The other present analyser module corresponds to the type 1219 from Bruel & Kjaer, and it is basically a heat stress monitor. Heat stress monitors are required in extreme indoor climates which can occur, for example, in ceramic industries due to the heat of the furnaces. Mainly, this type of monitor is the reference for environmental analysis in spaces where the operative temperature is higher than 30 °C and for these situations a new characterizing parameter is required: the WBGT. This acronym stands for Wet Bulb Globe Temperature and this depends on the measurement of 3 variables, the air and wet bulb temperatures and, most important, the Mean Radiant Temperature (MRT) (defined in the Appendix A), already referred to in this document. However, the present analyser module, in the current situation, only was used with the purpose to obtain and display the value of the globe temperature in order to, posteriorly, calculate the MRT.

As said before, the black globe is the one which is connected to the BK 1219 module through the WBGT set. This model of globe is a 150 mm diameter standard type, like the one it is possible to see on the Figure 0.9.



Figure 0.9. WBGT set of sensors (including the black globe).

This sensor consists of a matt black painted globe, generally made of copper (in sheet metal), which has placed, in its centre, a temperature sensor that can be a mercury thermometer, a thermocouple or a resistance probe. In the present work, the sensitive part is a PT100 resistance (RTD sensor). Black globes can have any diameters, but as the necessary formula to calculate the mean radiant temperature depends on the diameter, the normalized specified diameter for the globe attached to the BK 1219 is 150 millimeters (6 inches) [15]. It is necessary to note that the smaller the diameter of the globe, the more the air temperature and the air velocity are going to affect the globe temperature causing an accuracy reduction on the mean radiant temperature, as seen on the appendix A.

In conclusion, it is now possible to measure the MRT in the laboratory, however it is important to have in mind that the assessment to the mean radiant temperature by this

technique is an approximation, once the body of the instrument is a globe, and consequently not so closed to the human body shape. These type of globes, as standard, are optimum for experimental applications, but if it is necessary a constant monitoring and controlling solution in a complete and accessible radiant panel system, the solution wouldn't be the same. For that reason, in the present experimental activity, there are considered two extra black globes that can be locked on to a display system. These are not standard ones, instead they consist in PT1000 resistor temperature detectors in a pendulum shape, and have a diameter of 40 millimeters, as well as an emissivity of 0,92 according to the gloss paint coat instead of a matt one [16].

These globes are not connected to the BK1219 analyzer, but to the same DAQ board as the Swema anemometer sensor. The little black globe correspondent to the model RPF40 of Thermokon is presented in the following picture (Figure 0.10).



Figure 0.10. Thermokon's miniglobe.

Basically, the main difference between these little black globes and the standard one is that these two sensors, as already referred, are the most suitable solution for current contexts, having the possibility of connection to a single universal monitor and control module. Also, these globes are passive sensors, which means that the output energy becomes uniquely (or almost uniquely) from the input energy, whereby this is cheaper solution, just the right amount for a daily utilization.

Turning back to the BK1219 module, there is another radiant temperature sensor to consider, however this one sets in a different principle of work, as well, as a different analysis of the radiant exchanges from the surfaces. That instrument is the radiant temperature asymmetry transducer (also called net radiometer), which is represented in the next picture (Figure 6.11) as the type MM0036, and consists, not in a globe that reaches almost every possible directions, but in a two opposite and identical faces apparatus which

independently measures the irradiation on each plane (plane A or B as represented in the sensor).

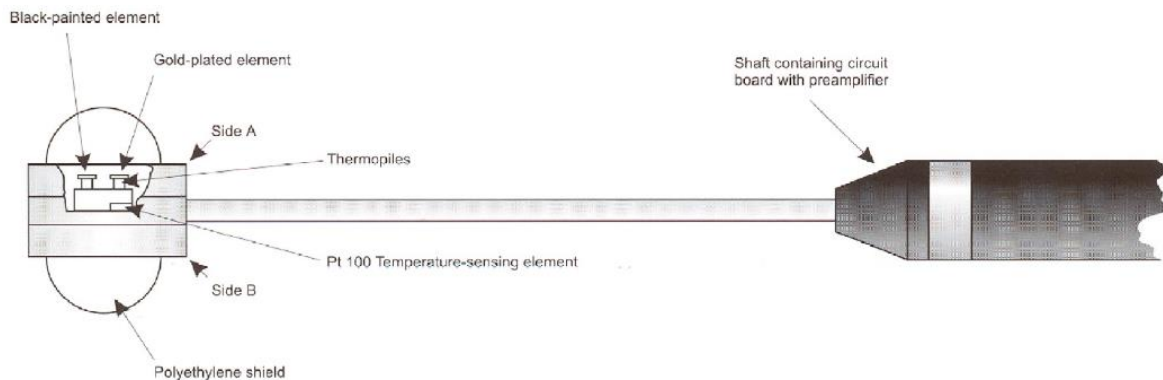


Figure 0.11. MM0036 temperature asymmetry transducer.

After all, a new concept is important in the experience, the Radiant Temperature Asymmetry (Δt_{pr}). This system variable is defined as the plane radiant temperature (t_{pr}) (which is defined in the Appendix A) difference between two opposite sides of a small black plane element. Following the same path, the plane radiant temperature is the result of heat radiation in one direction and can be defined as “the uniform surface temperature of a half room that produces the same incident radiation on a black surface as the actual environment” [14]. Besides measuring t_{pr} and Δt_{pr} , the net radiometer also has the possibility to measure the incident power which correspond to the value of the amount of radiation received, from the environment, by a black surface. Noting that, because the surface radiates itself (once it is above 0 kelvin), the quantity of received radiation is much lower than the incident power.

Each face of the transducer has a PT100 resistive temperature detector element and two elements of the same size, one black and one gold-plated that are connected to a centre block via thermopiles.

C – Calibrations and Adjustments

As explained in the Section 2.1.3, considering the first calibration procedure, the functions which represent the relation between each compared thermistor temperature and the reference thermistor temperature are represented in the graphic below (Figure 0.12), with the respective trend line and function.

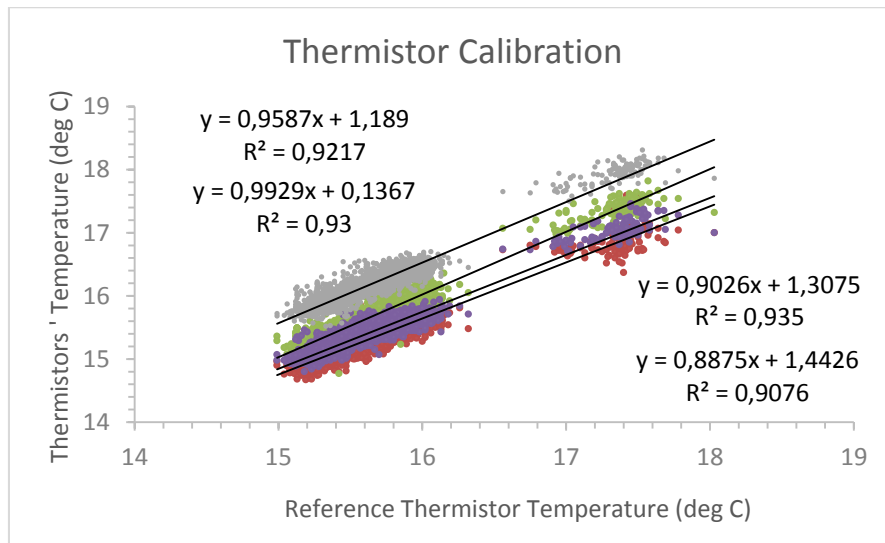


Figure 0.12. Thermistor calibration functions.

Note that y represents the compared thermistor temperature and the x the reference thermistor temperature (the number 3). Therefore, the present relations can be expressed by the following equations where T_i is the air temperature, in degrees Celsius, measured by the thermistor bar, with $i = 1,2,3,4$ and 5.

$$T_1 = 0,8875T_3 + 1,4426$$

$$T_2 = 0,9929T_3 + 0,1367$$

$$T_4 = 0,9026T_3 + 1,3075$$

$$T_5 = 0,9587T_3 + 1,189$$

Then, after calibration, the corrected temperature is represented by $T_{corr i}$. Following the explain method, the corrected measured temperatures become:

$$T_{corr 1} = \frac{T_1 - 1,4426}{0,8875}$$

$$T_{corr 2} = \frac{T_2 - 0,1367}{0,9929}$$

$$T_{corr 4} = \frac{T_4 - 1,3075}{0,9026}$$

$$T_{corr 3} = T_3$$

$$T_{corr 5} = \frac{T_5 - 1,189}{0,9587}$$

Continuing with the calibration procedures, in the adjustment of the miniglobes it was applied the same calibration method as the previous one as referred in the section (2.1.3). The functions correspondent the relation between each Thermokon globe

compared with the standard globe are, then, presented in the following graphic (Figure 0.13).

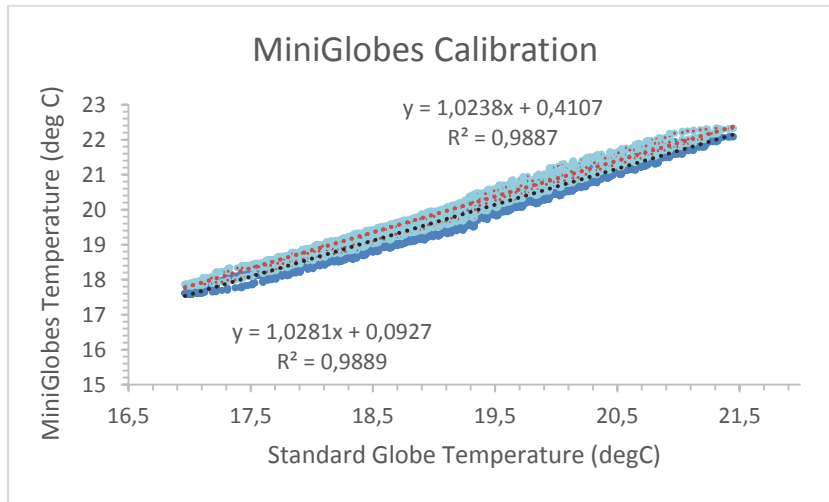


Figure 0.13. Miniglobes calibration functions.

Here, the darker colour belong to the miniglobe 1 and the lighter colour to the miniglobe 2; the y represents the miniglobes temperature and the x the reference black globe and the present relations can be expressed by the following equations where T_{g_i} is the globe temperature, in degrees Celsius, measured by each little black globe, with $i = 1$ and 2 , and $T_{g_{ref}}$ stands for the reference temperature of the standard globe.

$$T_{g_1} = 1,0281T_{g_{ref}} + 0,0927$$

$$T_{g_2} = 1,0238T_{g_{ref}} + 0,4107$$

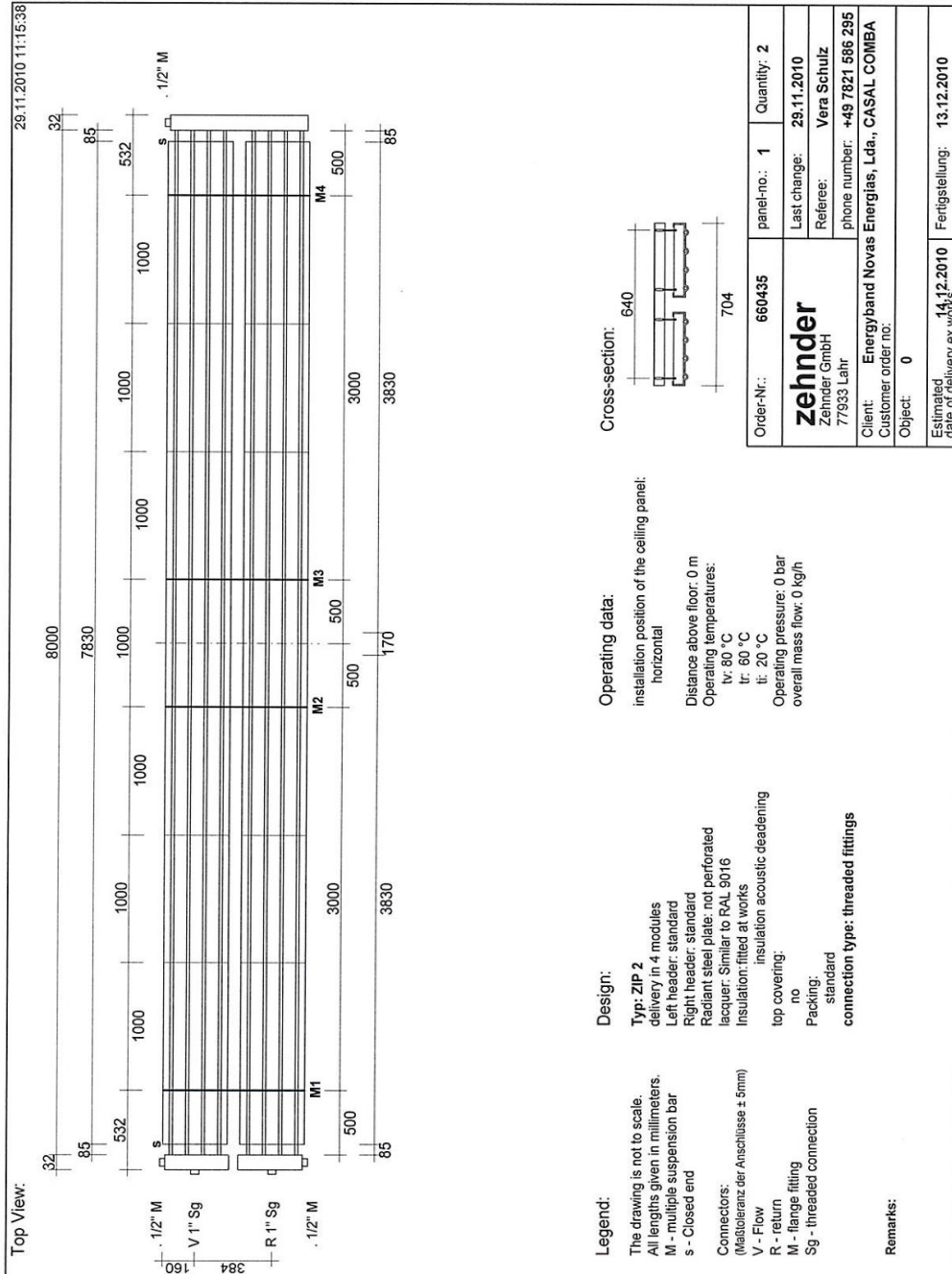
Following the calibration, the corrected temperatures are represented by $T_{g_{corr i}}$ and their calculation is defined next:

$$T_{g_{corr 1}} = \frac{T_{g_1} - 0,0927}{1,0281}$$

$$T_{g_{corr 2}} = \frac{T_{g_2} - 0,4107}{1,0238}$$

The results of the application of these calibration factors can be implicitly verified on the final data obtained in the experiment.

ANNEX A



ANNEX C

PMV_analysis.m

```
%PMV_analysis.m

A=dlmread("week1_1min_average_PMV_export_to_octave.txt",',',1,2); % read
"csv" delimited file
A=A(25:end,:);
T=A(:,4);
Pb=1013.25; %Barometric pressure in mbar
Ps=(1.0007+3.46e-6*Pb)*6.1121*exp((17.502*T)/(240.97+T));
RH=50; %assume nominal 50% relative humidity in the room
Pv=RH*Ps/100.0; %Partial pressure of water vapour (in mbar)

VEL=A(:,6);
TG=A(:,3);
TmG1=A(:,1);
TmG2=A(:,2);
OT=A(:,5);

P1=polyfit(TmG1,TG,1)
P2=polyfit(TmG2,TG,1)

TmG1=P1(1)*TmG1+P1(2); %recta de calibração:
TmG1,corr=0.96183TmG1+0.12035
TmG2=P2(1)*TmG2+P2(2); %recta de calibração: TmG2,corr=0.96565TmG2-
0.18264

Dmini=0.04;
epsilonmini=0.92;

Dg=0.15;
epsilong=0.95;

globe=0; %standard 150mm globe
D=Dg;
epsilon=epsilong;
hcn=1.4*(abs(TG-T)/D)^(1/4);
hcf=6.3*(VEL.^0.6)/D^0.4;
h=max([hcn hcf]');
mrT0=((TG+273).^4+0.25e+8/(epsilon*1.4).*h.*(TG-T)).^(1/4)-273;
[pmv0, ppd0]=PMV_calc(1,1.2,0,T,mrT0,VEL,Pv);
%operative temperature calculated:
sigma=5.67e-8 %Stefan-Boltzmann constant in W/(m2.K2)
feff=0.7; %ratio of radiating surface of the body to its total DuBois
area
hr=4*sigma*feff*((mrT0+T)/2+273).^3; %linear radiative heat transfer
coefficient W/(m2.K2)
hc=8.5*VEL.^0.5; %convective heat transfer coefficient
OT0=(hr.*mrT0+hc.*T)/(hr+hc);
```

```

globe=1;      %40mm mini-globe 1
D=Dmini;
epsilon=epsilonmini;
hcn=1.4*(abs(TmG1-T)/D).^(1/4);
hcf=6.3*(VEL.^0.6)/D^0.4;
h=max([hcn hcf]')';
mrT1=((TmG1+273).^4+0.25e+8/(epsilon*1.4).*h.*(TmG1-T)).^(1/4)-273;
[pmv1, ppd1]=PMV_calc(1,1.2,0,T,mrT1,VEL,Pv,globe);
%operative temperature calculated:
sigma=5.67e-8 %Stefan-Boltzmann constant in W/(m2.K2)
feff=0.7; %ratio of radiating surface of the body to its total DuBois
area
hr=4*sigma*feff*((mrT1+T)/2+273).^3; %linear radiative heat transfer
coefficient W/(m2.K2)
hc=8.5*VEL.^0.5; %convective heat transfer coefficient
OT1=(hr.*mrT1+hc.*T)./(hr+hc);

globe=2;      %40mm mini-globe 2
D=Dmini;
epsilon=epsilonmini;
hcn=1.4*(abs(TmG2-T)/D).^(1/4);
hcf=6.3*(VEL.^0.6)/D^0.4;
h=max([hcn hcf]')';
mrT2=((TmG2+273).^4+0.25e+8/(epsilon*1.4).*h.*(TmG2-T)).^(1/4)-273;
[pmv2, ppd2]=PMV_calc(1,1.2,0,T,mrT2,VEL,Pv,globe);
%operative temperature calculated:
sigma=5.67e-8 %Stefan-Boltzmann constant in W/(m2.K2)
feff=0.7; %ratio of radiating surface of the body to its total DuBois
area
hr=4*sigma*feff*((mrT2+T)/2+273).^3; %linear radiative heat transfer
coefficient W/(m2.K2)
hc=8.5*VEL.^0.5; %convective heat transfer coefficient
OT2=(hr.*mrT2+hc.*T)./(hr+hc);

B=[TmG1 TmG2 mrT0 OT0 pmv0 ppd0 mrT1 OT1 pmv1 ppd1 mrT2 OT2 pmv2 ppd2];

dlmwrite("thermal_comfort_results.txt",B,"delimiter",";","newline","pc");

figure
plot(TG,TmG1)
hold on

```

PMV_calc.m

```

%double compute_PMV(double CLO,double MET,double WME,double TA,double
TR,double VEL,double PA)
    %OCTAVE implementation of ISO7730:2005 Annex D program for
calculating PMV
    % Expected input units as follows:
    %
    %Input var      unit      Description
    % CLO           clo       Clothing
    % MET           met       Metabolic rate
    % WME           met       External work (normally around 0)
    % TA            degC      Air temperature
    % TR            degC      Mean radiant temperature
    % VEL           m/s       Relative(?) air velocity
    % PA            Pa        Water vapour pressure
    %
    % Alternatively, TA and TR can be both replaced by the Operative
Temperature, according
    % to the "Thermal Comfort" booklet by INNOVA, available online, e.g.
in (29/03/2015)
    %
http://www.labee.ufsc.br/antigo/arquivos/publicacoes/Thermal\_Booklet.pdf

function [pmv, ppd]=PMV_calc (CLO,MET,WME,TA,TR,VEL,PA)

    ICL=0.155*CLO
    M=MET*58.15
    W=WME*58.15
    MW=M-W

    if (ICL<=0.078)
        FCL=1.0+1.29*ICL;
    else
        FCL=1.05+0.645*ICL;
    endif

    HCF=12.1*sqrt (VEL);
    TAA=TA+273;
    TRA=TR+273;

    % calculate surface temperature of clothing by iteration
    TCLA=TAA+(35.5-TA) ./ (3.5*ICL+0.1);
    % printf("***Initial guess for TCL=%f\n",TCLA-273);
    P1=ICL.*FCL;
    P2=P1*3.96;
    P3=P1*100;
    P4=P1.*TAA;
    P5=308.7-0.028*MW+P2.*(TRA/100.0).^4;
    XN=TCLA/100.0;
    XF=XN;
    N=0;
    EPS=0.00015;
    ERRFLAG=0;
do

```

```

XF=(XF+XN)/2.0;
HCN=2.38.*abs(100.0*XF-TAA).^0.25;
if (HCF>HCN)
    HC=HCF;
else
    HC=HCN;
    XN=(P5+P4.*HC-P2.*XF.^4.0)./(100.0+P3.*HC);
    N=N+1;
    if (N>150)
        disp("*****Error in compute_PMV(): iteration did not converge
before MAXITER reached");
        ERRFLAG=1;
        break;
    endif
endif
until (abs(XN-XF)<=EPS)

if (ERRFLAG)
    PMV=999999;
else
    TCLA=100.0*XN;
    TCL=100.0*XN-273;
%    printf("***found TCL=%f; N=%d\n",TCL,N);
    HL1=3.05*0.001*(5733-6.99*MW-PA);
    if (MW>58.15)
        HL2=0.42*(MW-58.15);
    else HL2=0.0;
    endif
    HL3=1.7*0.00001*M.*(5867-PA);
    HL4=0.0014*M.*(34-TA);
    HL5=3.96e-8*FCL.*(TCLA.^4-TRA.^4);
    HL6=FCL.*HC.*(TCL-TA);
    TS=0.303*exp(-0.036*M)+0.028;
    PMV=TS.*(MW-HL1-HL2-HL3-HL4-HL5-HL6);
endif

pmv=PMV;
ppd=100-95*exp(-0.03353*pmv.^4-0.2179*pmv.^2);

endfunction

```

